



## Modeling the effects of tropospheric ozone on the growth and yield of global staple crops with DSSAT v4.8.0

Jose Rafael Guarin<sup>1,2,\*</sup>, Jonas Jägermeyr<sup>1,2</sup>, Elizabeth A. Ainsworth<sup>3</sup>, Fabio A. A. Oliveira<sup>4</sup>,  
Senthold Asseng<sup>5</sup>, Kenneth Boote<sup>4</sup>, Joshua Elliott<sup>6</sup>, Lisa Emberson<sup>7</sup>, Ian Foster<sup>8</sup>, Gerrit  
5 Hoogenboom<sup>4</sup>, David Kelly<sup>8</sup>, Alex C. Ruane<sup>2</sup>, Katrina Sharps<sup>9</sup>

<sup>1</sup>Center for Climate Systems Research, Columbia Climate School, Columbia University, New York, NY 10025 USA

<sup>2</sup>NASA Goddard Institute for Space Studies, New York, NY 10025 USA

<sup>3</sup>Global Change and Photosynthesis Research Unit, United States Department of Agriculture, Agricultural Research Service, Urbana, IL 61801

10 <sup>4</sup>Department of Agricultural and Biological Engineering, University of Florida, Gainesville, FL 32611 USA

<sup>5</sup>School of Life Sciences, HEF World Agricultural Systems Center, Technical University of Munich, Freising, 85354 Germany

<sup>6</sup>Center for Robust Decision-making on Climate and Energy Policy (RDCEP), University of Chicago, Chicago, IL 60637 USA

15 <sup>7</sup>Environment & Geography Dept., University of York, York, YO10 5NG UK

<sup>8</sup>Department of Computer Science, University of Chicago, Chicago, IL 60637 USA

<sup>9</sup>UK Centre for Ecology & Hydrology, Environment Centre Wales, Bangor, LL57 2UW, UK

\*Correspondence to: Jose Rafael Guarin ([j.guarin@columbia.edu](mailto:j.guarin@columbia.edu))

### Highlights

- 20
- Effects of O<sub>3</sub> stress on photosynthesis and leaf senescence were added to the DSSAT/pDSSAT maize, rice, soybean, and wheat crop models.
  - The modified models reproduced growth and yields under different O<sub>3</sub> levels observed in field experiments and reported in the literature.
  - Expected detrimental interactions between O<sub>3</sub>, CO<sub>2</sub>, and water deficit were reproduced with the new models.
- 25
- The updated crop models can be used to simulate impacts of O<sub>3</sub> stress under future climate change and air pollution scenarios.

**Abstract.** Elevated surface ozone (O<sub>3</sub>) concentrations can negatively impact growth and development of crop production by reducing photosynthesis and accelerating leaf senescence. Under unabated climate change, future global O<sub>3</sub> concentrations are expected to increase in many regions, adding additional challenges to global agricultural production. Presently, few global process-based crop models consider the effects of O<sub>3</sub> stress on crop growth. Here, we incorporated the effects of O<sub>3</sub> stress on photosynthesis and leaf senescence into the Decision Support System for Agrotechnology Transfer (DSSAT) crop models for maize, rice, soybean, and wheat. The advanced models reproduced the reported yield declines from observed O<sub>3</sub>-dose field experiments and O<sub>3</sub> exposure responses reported in the literature (O<sub>3</sub> relative yield loss RMSE < 10% across all calibrated models). Simulated crop yields decreased as daily O<sub>3</sub> concentrations increased above 25 ppb, with average yield losses of 0.16% to 0.82% (maize), 0.05% to 0.63% (rice), 0.36% to 0.96% (soybean), and 0.26% to 1.23% (wheat) per ppb O<sub>3</sub> increase, depending on the cultivar O<sub>3</sub> sensitivity. Increased water deficit stress and elevated CO<sub>2</sub> lessen the negative impact of elevated O<sub>3</sub> on crop yield,

30

35



but potential yield gains from CO<sub>2</sub> concentration increases may be counteracted by higher O<sub>3</sub> concentrations in the future, a potentially important constraint to global change projections for the latest process-based crop models. The improved DSSAT models with O<sub>3</sub> representation simulate the effects of O<sub>3</sub> stress on crop growth and yield in interaction with other growth factors and can be run in the parallel DSSAT global gridded modeling framework for future studies on O<sub>3</sub> impacts under climate change and air pollution scenarios across agroecosystems globally.

### Keywords

Surface ozone, climate change, global process-based crop model, phytotoxicity, staple crop yield

## 1 Introduction

Surface or ground-level, ozone (O<sub>3</sub>) is a major air pollutant that causes adverse impacts on agricultural productivity worldwide (Mills et al., 2018b; Emberson et al., 2018; Tai et al., 2021). O<sub>3</sub> is formed through photochemical reactions between incoming solar radiation and primary pollutants such as Nitrogen Oxides (NO<sub>x</sub> = NO + NO<sub>2</sub>), Volatile Organic Compounds (VOCs), Carbon Monoxide (CO), or Methane (CH<sub>4</sub>) across all areas of the globe (Cooper et al., 2014; Simpson et al., 2014). Global O<sub>3</sub> concentrations have increased 2-7% per decade in northern mid-latitude regions and 2-12% per decade in tropical regions since the mid-1990s (Ipcc, 2021; Arias et al., 2021). Future O<sub>3</sub> concentrations are projected to continue increasing if O<sub>3</sub> precursor emissions are not mitigated, i.e., following the shared socio-economic pathways where regional rivalry leads to doubling of CO<sub>2</sub> emissions by 2100 (SSP3-7.0) or where fossil fuel enabled growth leads to doubling of CO<sub>2</sub> emissions by 2050 (SSP5-8.5) (Ipcc, 2021; Arias et al., 2021; Szopa et al., 2021; Griffiths et al., 2021).

Crops exposed to elevated levels of O<sub>3</sub> concentrations can experience reduced photosynthesis, accelerated senescence, foliar chlorosis and even necrosis from increased cumulative oxidative stress (Ainsworth, 2017). These negative effects lead to decreased productivity resulting in global yield losses between 2-16% for the four main staple crops: maize, rice, soybean, and wheat (Ainsworth, 2017; Schiferl and Heald, 2018; Emberson, 2020), with global annual economic damages of approximately \$34 billion (Sampedro et al., 2020; Feng et al., 2022). Climate change may exacerbate the negative effects from elevated O<sub>3</sub> concentrations because O<sub>3</sub> concentrations are highest in summer months and the projected higher temperatures with more frequent heat waves may lead to a longer period of more active photochemical reactions (Zhang and Wang, 2016; Hou and Wu, 2016; Szopa et al., 2021). Elevated concentrations of atmospheric CO<sub>2</sub> and increased periods of water deficit stress cause stomatal closure that can reduce crop O<sub>3</sub> uptake (Khan and Soja, 2003; Biswas et al., 2013), but in turn potential yield gains associated with the CO<sub>2</sub> fertilization effect (Toreti et al., 2020; Jagermeyr et al., 2021) may be constrained by elevated O<sub>3</sub>. Therefore, it is important to evaluate net O<sub>3</sub> effects for crop growth and consider the effects of O<sub>3</sub> in global agricultural assessments examining future scenarios.

Process-based crop simulation models have been used to evaluate the impacts of O<sub>3</sub> on crop yields (Guarin et al., 2019; Tai et al., 2021), but most global gridded process-based crop models are still unable to respond to O<sub>3</sub> stress. Recently, the global Lund-Potsdam-Jena managed Land (LPJmL) and Joint UK Land Environment Simulator



(JULES) models were modified to include the effects of O<sub>3</sub> stress on soybean and wheat growth (Schauberger et al., 2019; Leung et al., 2020). Additionally, the Agricultural Model Intercomparison and Improvement Project (AgMIP; Rosenzweig et al. (2013)) Ozone Team has recently developed protocols for incorporating O<sub>3</sub> stress into a wider body  
75 of crop models aiming to establish the first multi-model assessment of ozone impacts in agriculture at global level (Emberson et al., 2018).

The aim of this study is to incorporate the effects of O<sub>3</sub> concentrations into the stress response functions of the maize, rice, soybean, and wheat models within the established Decision Support System for Agrotechnology Transfer (DSSAT) v4.8.0 modeling platform (Jones et al., 2003; Hoogenboom et al., 2019), and consequently the parallel  
80 DSSAT (pDSSAT) v4.8.0 global gridded modeling platform that is used to run DSSAT in a global setup (Elliott et al., 2014), to simulate O<sub>3</sub> effects on global crop development and yield for the four major staple crops. The observational data from the Free-air CO<sub>2</sub> Enrichment (FACE) field experiments conducted in Champaign, Illinois, USA (Choquette et al., 2020; Betzelberger et al., 2012) and well-known O<sub>3</sub> exposure relationships reported in the literature are used to develop and calibrate the model O<sub>3</sub> response functions. Additionally, the observed interactions  
85 between O<sub>3</sub>, CO<sub>2</sub>, and water deficit stress are examined via sensitivity analyses conducted with the modified models.

## 2 Materials and Methods

### 2.1 Description of crop models

The crop models within the pDSSAT parallel modeling environment are based on the existing crop models within the widely used DSSAT crop modeling platform (Jones et al., 2003; Hoogenboom et al., 2019) combined with the Center  
90 for Robust-Decision Making on Climate and Energy Policy (RDCEP) Parallel System for Integrating Impact Models and Sectors (pSIMS) framework (Elliott et al., 2014) to allow for global gridded process-based crop modeling on high performance computational systems. The O<sub>3</sub> stress routines presented here are also applied in the standard DSSAT crop models and can be used for field level simulations and point-based testing in addition to the global-level modeling applications.

95 The four DSSAT crop models used in this study are the Crop Environment Resource Synthesis (CERES) -Maize, CERES-Rice, Crop Growth Simulation (CROPGRO) -Soybean, and Nitrogen Wheat (NWheat) models that have been used in previous AgMIP crop model intercomparisons (Bassu et al., 2014; Li et al., 2015; Asseng et al., 2015; Kothari et al., 2022). The CERES-Maize and CERES-Rice models were previously used to estimate global ozone crop losses (Schiferl and Heald, 2018); however, their approach was based on the multiplication of the simulated global base  
100 production by the relative yield-O<sub>3</sub> response functions to determine a response proxy. The approach used in this present study integrates daily process-based stress calculations to simulate daily crop growth and stress dynamics. Thus, the models are more applicable to a much broader range of scenarios given that they can combine daily stress interactions and can be used to scale across agroecosystems in a more robust way.

### 2.2 O<sub>3</sub> incorporation into the crop models



105 The incorporation of O<sub>3</sub> effects into the DSSAT crop models followed the same methodology as the O<sub>3</sub> incorporation  
into the DSSAT-NWheat crop model (Guarin et al., 2019). O<sub>3</sub> response was added to the models via the inclusion of  
daily photosynthesis reduction and leaf senescence acceleration functions. Additionally, the interaction between O<sub>3</sub>  
and water deficit stress and/or atmospheric CO<sub>2</sub> concentrations was incorporated into the models since these combined  
110 interactions can mitigate impacts from O<sub>3</sub> on crop production and vice-versa. For example, water deficit stress that  
induces stomatal closure in turn limits O<sub>3</sub> stress because of reduced aerosol uptake (Khan and Soja, 2003; Biswas et  
al., 2013).

### 2.2.1 CERES-Maize and CERES-Rice models

The effects of O<sub>3</sub> were incorporated into the CERES-Maize and CERES-Rice models using similar methodology since  
these two models share similar code. O<sub>3</sub> was added into the models using a photosynthesis reduction stress factor  
115 (FO<sub>3</sub>) following Eq. (1):

$$FO_3 = \max\left(0.0, -\left(\frac{FOZ_1}{100}\right) * OZON_7 + \left(1.0 + \left(\frac{FOZ_1}{100}\right) * 25.0\right)\right), \quad (1)$$

where OZON<sub>7</sub> is the daily mean 7-hour (M7, 9:00 – 15:59 hr) O<sub>3</sub> concentration (ppb) and FOZ<sub>1</sub> is the O<sub>3</sub> stress  
parameter for photosynthesis calibrated for different O<sub>3</sub> sensitivities of cultivars divided by a decimal correction factor  
of 100. The decimal correction factor ensures that the FOZ<sub>1</sub> parameter value ranges between 0.0 and 1.0 in the model  
120 ecotype parameter file for comprehensible user input. A minimum M7 O<sub>3</sub> threshold of 25 ppb was set as the reference  
value based on pre-industrial O<sub>3</sub> concentrations and the United States National Crop Loss Assessment Network  
(NCLAN) studies indicating that O<sub>3</sub> damage within crops occurs above this threshold (Heck et al., 1984; Lesser et al.,  
1990; Feng and Kobayashi, 2009). When the daily M7 O<sub>3</sub> concentration exceeds this threshold, photosynthesis is  
reduced by a factor between 0.0 to 1.0 (Eq. (1)) and leaf senescence is accelerated by a factor between 0.0 to 1.0 (Eq.  
125 (5)).

Eq. (1) does not include the interaction of O<sub>3</sub> stress with water deficit stress or elevated atmospheric CO<sub>2</sub>. To consider  
these combined interactions on crop growth (PRFO<sub>3</sub>), FO<sub>3</sub> was modified using Eq. (2):

$$PRFO_3 = \min\left(1.0, \left(\frac{FO_3 * PCO_2}{SWFAC}\right)\right), \quad (2)$$

where PCO<sub>2</sub> is the atmospheric CO<sub>2</sub> effect on potential daily dry matter production and SWFAC is the water stress  
130 factor on photosynthesis (Jones and Kiniry, 1986; Ritchie et al., 1987; Jones et al., 2003). Since PCO<sub>2</sub> is always greater  
than one, multiplying by the CO<sub>2</sub> effect mitigates the reduction caused by FO<sub>3</sub>. Because SWFAC is a reduction factor  
between zero and one, dividing by this factor decreases the reduction from FO<sub>3</sub> under increased water deficit stress  
conditions.

The simulated daily biomass production (CARBO, g plant<sup>-1</sup> day<sup>-1</sup>) within the models was calculated based on the  
135 existing photosynthesis stress factors with the addition of PRFO<sub>3</sub> using Eq. (3) for maize and Eq. (4) for rice:

$$CARBO_{maize} = PCARB * \min(PRFT, SWFAC, NSTRES, PSTRES_1, KSTRES, PRFO_3) * SLPF, \quad (3)$$

$$CARBO_{rice} = PCARB * \min(PRFT, SWFAC, NSTRES, TSHOCK, PSTRES_1, KSTRES, PRFO_3) * SLPF, \quad (4)$$



where PCARB is daily potential dry matter production of the crop accounting for light interception, radiation use efficiency, and the CO<sub>2</sub> effect on photosynthesis (g plant<sup>-1</sup>), PRFT, SWFAC, NSTRES, TSHOCK (CERES-Rice only),  
 140 PSTRES<sub>1</sub>, KSTRES, and PRFO<sub>3</sub> are the temperature, soil water, Nitrogen, transplanting shock, Phosphorous, Potassium, and O<sub>3</sub> stress factors on photosynthesis, respectively, and SLPF is the soil fertility factor (Jones and Kiniry, 1986; Ritchie et al., 1987; Jones et al., 2003).

Leaf senescence acceleration due to O<sub>3</sub> stress (SLFO<sub>3</sub>) was added to the models using Eq. (5):

$$145 \quad SLFO_3 = \max\left(0.0, -\left(\frac{SFOZ_1}{1000}\right) * OZON_7 + \left(1.0 + \left(\frac{SFOZ_1}{1000}\right) * 25.0\right)\right), \quad (5)$$

where SFOZ<sub>1</sub> is the O<sub>3</sub> stress parameter for leaf senescence calibrated for different O<sub>3</sub> sensitivities of cultivars divided by a decimal correction factor of 1000 (to ensure the SFOZ<sub>1</sub> parameter value ranges between 0.0 and 1.0 in the model ecotype file). The SLFO<sub>3</sub> factor was then included in the existing daily rate of leaf area senescence function (PLAS, cm<sup>2</sup> day<sup>-1</sup>) within the models as shown in Eq. (6) for maize and Eq. (7) for rice:

$$150 \quad PLAS_{maize} = (PLA - SENLA) * \left(1 - \min(SLFW, SLFC, SLFT, SLFN, SLFP, SLFO_3)\right), \quad (6)$$

$$PLAS_{rice} = (PLA - SENLA) * \left(1 - \min(SLFW, SLFC, SLFT, SLFN, SLFP, SLFK, SLFO_3)\right), \quad (7)$$

where PLA is daily plant leaf area (cm<sup>2</sup> plant<sup>-1</sup>), SENLA is daily normal leaf senescence (cm<sup>2</sup> plant<sup>-1</sup>), and SLFW, SLFC, SLFT, SLFN, SLFP, SLFK, and SLFO<sub>3</sub> are the leaf senescence stress factors due to water, light competition, temperature, Nitrogen, Phosphorous, Potassium (CERES-Rice only), and O<sub>3</sub> stress, respectively (Jones and Kiniry,  
 155 1986; Ritchie et al., 1987; Jones et al., 2003).

## 2.2.2 CROPGRO-Soybean model

The effects of O<sub>3</sub> were incorporated into the CROPGRO-Soybean model using a similar approach as described in the CERES crop models. O<sub>3</sub> was added into the model using the same FO<sub>3</sub> and PRFO<sub>3</sub> factors as in Eq. (1) and Eq. (2) (for Eq. (2), PCO<sub>2</sub> is called PRATIO in CROPGRO-Soybean). However, CROPGRO-Soybean calculates daily  
 160 photosynthesis differently than the other models and has two different photosynthesis calculation options, leaf or canopy photosynthesis (Wilkerson et al., 1983; Boote and Pickering, 1994; Jones et al., 2003). This study focuses on the default leaf photosynthesis calculation option (which was modified to read in the CO<sub>2</sub> ratio effect for the PRFO<sub>3</sub> interaction). The daily gross photosynthesis (PG, g [CH<sub>2</sub>O] m<sup>-2</sup> day<sup>-1</sup>) within the model was calculated based on the limiting photosynthesis stress factors using Eq. (8) for leaf photosynthesis and Eq. (9) for canopy photosynthesis:

$$165 \quad PG_{leaf} = \left(\frac{PGDAY}{44.0} * 30.0 * SLPF\right) * \min(SWFAC, PRFO_3) * PSTRES_1, \quad (8)$$

$$PG_{canopy} = PTSMAX * SLPF * PG_{FAC} * TPG_{FAC} * E_{FAC} * PG_{SLW} * PRATIO * PGLFMX * \min(SWFAC, PRFO_3), \quad (9)$$

where PGDAY is daily potential photosynthesis (g [CH<sub>2</sub>O] m<sup>-2</sup> day<sup>-1</sup>), SWFAC, PSTRES<sub>1</sub>, and PRFO<sub>3</sub> are the soil water, Phosphorous, and O<sub>3</sub> stress factors on photosynthesis, respectively. PTSMAX is the potential amount of CH<sub>2</sub>O that can be produced for the full canopy (g [CH<sub>2</sub>O] m<sup>-2</sup> day<sup>-1</sup>), PG<sub>FAC</sub> is a factor to compute daily PG as a function of



170 leaf area index,  $TPG_{FAC}$  is a reduction factor for specific leaf area due to less optimal daytime temperature,  $E_{FAC}$  is the effect of Nitrogen and Phosphorous stress on daily canopy photosynthesis,  $PGSLW$  is the relative effect of leaf thickness on daily canopy photosynthesis, and  $PRATIO$  is the relative effect of atmospheric  $CO_2$  on daily canopy photosynthesis (Boote and Pickering, 1994).

Leaf senescence acceleration due to  $O_3$  stress ( $SLFO_3$ ) was added to CROPGRO-Soybean using Eq. (10):

$$175 \quad SLFO_3 = \max\left(0.0, \left(\frac{SFOZ_1}{1000}\right) * OZON_7 - \left(\left(\frac{SFOZ_1}{1000}\right) * 25.0\right) * WTLF\right), \quad (10)$$

where  $WTLF$  is the dry mass of leaf tissue ( $g_{leaf} m^{-2}$ ). The CROPGRO leaf senescence routine is based on increasing  $WTLF$ , which is different from the CERES leaf senescence reduction factor, so  $SLFO_3$  has the opposite trend when compared to the CERES model calculation (Fig. 1). The  $SLFO_3$  factor was then included in the existing daily defoliation due to daily leaf senescence ( $SLDOT$ ,  $g m^{-2} day^{-1}$ ) calculation within the model as shown in Eq. (11):

$$180 \quad SLDOT = SLDOT_n + \max(SLNDOT, SLFO_3), \quad (11)$$

where  $SLDOT_n$  is the natural daily leaf senescence and  $SLNDOT$  and  $SLFO_3$  are the daily leaf senescence due to water and  $O_3$  stress ( $g m^{-2} day^{-1}$ ), respectively.

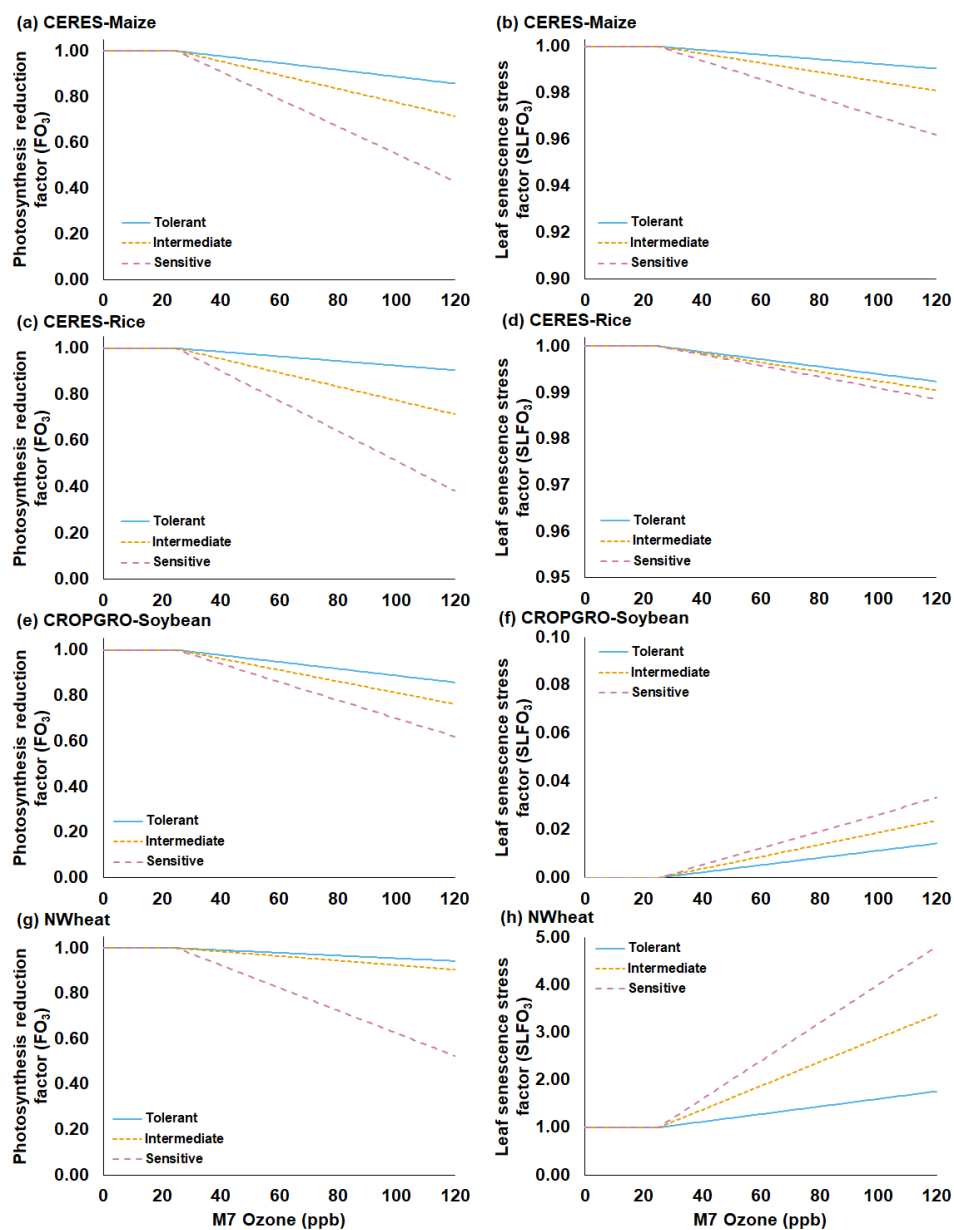
### 2.2.3 DSSAT-NWheat model

185 The incorporation of  $O_3$  into the NWheat crop model was described and validated in Guarin et al., (2019) and was used as the reference for the maize, rice, and soybean models. The approach used the same  $FO_3$  and  $PRFO_3$  equations as in Eq. (1) and (2) (note that the NWheat equations were simplified from Guarin et al., (2019) by the decimal correction factor and single  $FOZ_1$  parameter as in Eq. (1) for consistency among all models) and a similar  $SLFO_3$  shown in Eq. (12):

$$SLFO_3 = \left(\frac{SFOZ_1}{10}\right) * OZON_7 + \left(1.0 - \left(\frac{SFOZ_1}{10} * 25.0\right)\right). \quad (12)$$

190 The  $O_3$  effect for the different cultivar sensitivities is controlled by the  $FOZ_1$  and  $SFOZ_1$  parameters, as in the other models (the  $SFOZ_1$  parameter is divided by 10 to ensure that the value ranges between 0.0 and 1.0 in the model ecotype file). The decimal correction factors vary between the crop models because the different models calculate stresses using different magnitudes.

195 The  $FO_3$  and  $SLFO_3$  responses calculated over increasing  $M7 O_3$  concentrations are illustrated for each model in Fig. 1 using the parameter values for different  $O_3$  cultivar classifications shown in Table 1. The  $FOZ_1$  and  $SFOZ_1$  parameter values for all models were determined from the cultivar sensitivities observed in the field experiments (section 2.3) and the sensitivities derived from the  $O_3$  exposure relationships from the literature (section 2.5).



200 Figure 1: Functions for the O<sub>3</sub> photosynthesis reduction factor without interaction of water deficit stress and CO<sub>2</sub>  
 fertilization effect (FO<sub>3</sub>) (first column) and the O<sub>3</sub> leaf senescence acceleration stress factor (SLFO<sub>3</sub>) (second column) under  
 increasing mean 7-hour (M7) O<sub>3</sub> concentrations for the (a, b) CERES-Maize, (c, d) CERES-Rice, (e, f) CROPGRO-Soybean,  
 205 and (g, h) NWheat models. Each figure shows three different O<sub>3</sub> sensitivity cultivar classifications derived from the O<sub>3</sub>  
 exposure-yield responses from the literature: tolerant (blue solid line), intermediate (gold short-dash line), and sensitive  
 (magenta long-dash line). SLFO<sub>3</sub> for CROPGRO-Soybean (Eq. (10)) shown with leaf tissue dry mass (WTLF) of 1 g m<sup>-2</sup> for  
 simplicity. Steeper slopes indicate a higher sensitivity to O<sub>3</sub> for both FO<sub>3</sub> and SLFO<sub>3</sub>. Table 1 shows the parameters used in  
 the equations for each classification of O<sub>3</sub> sensitivity (Eq. (1), (5), (10), and (12)).





210 **Table 1: Summary of the O<sub>3</sub> photosynthesis stress parameters (FOZ<sub>1</sub>) and the O<sub>3</sub> leaf senescence stress parameters (SFOZ<sub>1</sub>) used in the FO<sub>3</sub> and SLFO<sub>3</sub> calculations (Eq. (1), (5), (10), and (12)) for the four DSSAT models under three different O<sub>3</sub> sensitivity cultivar classifications. The CERES and CROPGRO parameter values were determined from the O<sub>3</sub> exposure-yield responses in the literature (Fig. S2, Fig. S3). NWheat parameter values were from Guarin et al., (2019) and confirmed with the literature.**

O <sub>3</sub> sensitivity cultivar classifications	CERES-Maize		CERES-Rice		CROPGRO-Soybean		NWheat	
	FOZ <sub>1</sub>	SFOZ <sub>1</sub>	FOZ <sub>1</sub>	SFOZ <sub>1</sub>	FOZ <sub>1</sub>	SFOZ <sub>1</sub>	FOZ <sub>1</sub>	SFOZ <sub>1</sub>
Tolerant	0.15	0.10	0.10	0.08	0.15	0.15	0.06	0.08
Intermediate	0.30	0.20	0.30	0.10	0.25	0.25	0.10	0.25
Sensitive	0.60	0.40	0.65	0.12	0.40	0.35	0.50	0.40

### 215 2.3 Observed O<sub>3</sub> exposure field experiments

In general, detailed field experiments of crop growth under elevated O<sub>3</sub> conditions for different crops are scarce and limit the granularity of model calibration. All field experiments examined in this study used dominant management conditions to limit other stresses besides O<sub>3</sub>, e.g., water deficit or N stress, so the simulations assumed negligible outside stresses.

220 For maize, the FACE experiment conducted at Champaign, Illinois, USA (40.03 °N, 88.27 °W, 230 m elevation) in 2018 was used for calibrating the CERES-Maize model (Choquette et al., 2020). The maize FACE experiment consisted of six cultivars grown under an ambient and an elevated O<sub>3</sub> treatment with  $n = 4$  (Table 2). Since there was only one year of data, the model was validated against the O<sub>3</sub> exposure-relative yield response functions from the literature (section 2.5). The daily maximum temperature (TMAX), minimum temperature (TMIN), and precipitation

225 (RAIN) weather data were collected from the nearby National Oceanic and Atmospheric Administration (NOAA) Willard airport weather station and the daily incoming solar radiation (SRAD) was collected from the National Aeronautics and Space Administration (NASA) Prediction Of Worldwide Energy Resources (POWER) database (<https://power.larc.nasa.gov/>). The soil consisted of the Drummer silty clay loam soil series, and the soil parameters for this series were obtained from the United States Department of Agriculture (USDA) Natural Resources

230 Conservation Service (NRCS) Web Soil Survey database (Table S1) (Nrcs, 2023). The cultivars were planted in two 3.5 m rows with a row spacing of 0.76 m on May 13, 2018 (Choquette et al., 2020). The hourly O<sub>3</sub> fumigation (from 10:00 to 18:00) began on May 25, 2018 and ended on August 14, 2018 and was used to calculate the daily M7 O<sub>3</sub> concentrations. The cultivar plots were harvested at maturity on September 21, 2018. N and water deficit stress were reported to be non-limiting, so the simulations used the non-limiting N setting within the model and the simulated

235 water stress was confirmed to be non-limiting with the provided rainfall. The DSSAT cultivar parameters were calibrated for phenology and growth under negligible stress conditions using the treatment with the ambient O<sub>3</sub> concentration (38 ppb) for each cultivar. After the phenology and growth cultivar parameters were calibrated, the FOZ<sub>1</sub> and SFOZ<sub>1</sub> O<sub>3</sub> response parameters were calibrated using the yield response from the elevated O<sub>3</sub> concentration treatments (Fig. S1 (a)).

240 For soybean, data from the FACE experiment conducted at the same location in Champaign, Illinois, USA (40.03 °N, 88.27 °W, 230 m elevation) in 2009 and 2010 was used for model testing (Betzberger et al., 2012). The 2009 data was used for model calibration and the 2010 data was used for model validation. These data were previously used to





incorporate O<sub>3</sub> effects on leaf photosynthesis into the JULES model (Leung et al., 2020). The SoyFACE experiment consisted of seven soybean cultivars grown under nine O<sub>3</sub> treatments with different target concentrations (Table 2).  
 245 The hourly O<sub>3</sub> fumigation data (plots fumigated for 8 to 9 hours daily except when leaves were wet) for each treatment was recorded in situ and was used to calculate the daily M7 O<sub>3</sub> concentrations (Betzelberger et al., 2012). The weather data was collected from the same sources as used in the maize experiment (NOAA and NASA POWER), and the soil consisted of either the Drummer silty clay loam or the Flanagan silt loam series which were obtained from the USDA NRCS Web Soil Survey database (Table S1). The initial soil conditions of the simulations were set at 95% available  
 250 water content and 100 kg N ha<sup>-1</sup> to minimize water and N stress. The cultivars were planted in plots eight rows wide and 5.4 m long, with a row spacing of 0.38 m, on June 9, 2009 and May 27, 2010. The O<sub>3</sub> fumigation started on June 29, 2009 and June 6, 2010, and ended on September 27, 2009 and September 17, 2010. The cultivar plots were harvested at maturity on October 20, 2009 and September 30, 2010. For each specified cultivar maturity group (Betzelberger et al., 2012), the corresponding default DSSAT maturity group parameters were used as reference and  
 255 then calibrated for phenology and growth under negligible stress using the treatment with the ambient O<sub>3</sub> concentration (37 ppb). After the phenology and growth cultivar parameters were calibrated, the FOZ<sub>1</sub> and SFOZ<sub>1</sub> O<sub>3</sub> response parameters were calibrated using the yield response from the elevated O<sub>3</sub> concentration treatments (Fig. S1 (b)). The parameters for both maize and soybean were calibrated using the using the one-factor-at-at-time method (Morris, 1991) until the best fit was found for the phenology, growth, and relative yield loss for each cultivar across all O<sub>3</sub>  
 260 treatments.

**Table 2: O<sub>3</sub> fumigation target concentration and average mean 7-hour (M7, 9:00 – 15:59 hr) O<sub>3</sub> concentrations for the 2018 maize FACE experiment (Choquette et al., 2020) and the 2009 and 2010 soybean SoyFACE experiments (Betzelberger et al., 2012).**

Crop experiment	O <sub>3</sub> fumigation target concentration (ppb)	Average M7 O <sub>3</sub> concentration (ppb)
Maize 2018	Ambient	38
	100	77
Soybean 2009	Ambient	37
	40	39
	55	47
	70	57
	85	61
	110	75
	130	96
	160	102
	200	126
Soybean 2010	Ambient	37
	55	46
	70	52
	85	59
	110	69
	130	76
	150	70
	170	84
	190	84



265

For rice, there was no O<sub>3</sub> field experiment data readily available, thus a representative rice-producing location in the main North American rice-producing area at Stuttgart, Arkansas, USA (34.50 °N, 91.55 °W, 60 m elevation) (Usda Nass, 2010) was simulated with the default DSSAT North American rice cultivar. 2009 was selected for consistency with the soybean simulations. The weather data was collected from the NASA POWER database and the dominant soil series for Arkansas County, Dewitt silt loam, was determined from the USDA NRCS Web Soil Survey database (Table S1) (Nrcs, 2023). The initial soil conditions of the simulations were set at 100% available water content and 100 kg N ha<sup>-1</sup> to ensure negligible water and N stress. Four 50 kg N ha<sup>-1</sup> fertilizer applications were applied throughout the season to ensure negligible N stress in the simulations. The cultivar was planted on April 20, 2009 based on the most active planting dates recorded for Arkansas in the USDA Field Crops handbook (Usda Nass, 2010), and the harvest date was automatically calculated based on when the model simulations reached physiological maturity. The default DSSAT North American rice cultivar parameters were used, and the FOZ<sub>1</sub> and SFOZ<sub>1</sub> O<sub>3</sub> response parameters were calibrated using the yield response from the elevated O<sub>3</sub> exposure functions from the literature (section 2.5).

270

275

For wheat, the NWheat model was calibrated and validated using an air exclusion system O<sub>3</sub> exposure wheat field experiment conducted in Wake County, North Carolina, USA (35.73 °N, 78.68 °W, 116 m elevation) and is described in detail in Guarin et al., (2019).

280

#### 2.4 Sensitivity analysis of O<sub>3</sub> equations and parameters

A sensitivity analysis for maize, rice, and soybean was conducted using simulations of nine constant daily M7 O<sub>3</sub> concentrations of 25, 40, 50, 60, 70, 80, 90, 100, and 120 ppb with different FOZ<sub>1</sub> and SFOZ<sub>1</sub> parameter values under combinations between normal or 50% reduced rainfall and 350 ppm or 550 ppm CO<sub>2</sub> concentrations to confirm that the O<sub>3</sub> modifications and stress interactions within the models were behaving as expected. The simulated locations and management setup for each crop were the same as the field experiments described above (section 2.3). For wheat, the sensitivity analysis was based on the 1993 FACE experiment conducted in Maricopa, Arizona (33.06 °N, 111.98 °W, 361 m elevation) (Hunsaker et al., 1996; Kimball et al., 1999; Kimball et al., 2017). The simulation setup for the Maricopa FACE experiment used the same 9 M7 O<sub>3</sub> concentrations with either a “Wet” irrigation schedule (total of 629 mm sub-surface drip irrigation at 0.23 m from planting to harvest) or a “Dry” irrigation schedule (total of 347 mm sub-surface drip irrigation at 0.23 m from planting to harvest) under 350 ppm and 550 ppm CO<sub>2</sub> concentrations to examine the O<sub>3</sub>-CO<sub>2</sub>-water interactions as detailed in Guarin et al., (2019). For all crops, each O<sub>3</sub> parameter was first tested independently to examine the individual effects on photosynthesis and leaf senescence, i.e., when examining FOZ<sub>1</sub>, SFOZ<sub>1</sub> was set to zero and vice versa.

285

290

295

#### 2.5 Observed O<sub>3</sub> exposure relationships based on the literature

To confirm that the models were able to reproduce the observed relative yield loss due to O<sub>3</sub> stress, the simulated results were compared to well-known literature reports of O<sub>3</sub> exposure metrics and yield response for each crop using the M7 O<sub>3</sub> concentrations. The simulated locations and management conditions were the same experimental conditions as described above for each crop. For each crop, different O<sub>3</sub> classification of cultivar sensitivities were defined based



300 on more severe response to O<sub>3</sub> stress, i.e., tolerant, intermediate, and sensitive. These classifications of cultivar O<sub>3</sub>  
sensitivity were determined using the extensive literature review data from Mills et al. (2018a) combined with the  
maize and soybean FACE data for a total of 9 maize cultivars, 50 rice cultivars, 49 soybean cultivars, and 23 wheat  
cultivars. The literature review consisted of O<sub>3</sub> exposure experiments conducted in open-top chambers, experimental  
305 fields, or greenhouses and included the experiments that contributed to the widely applied Weibull O<sub>3</sub> response  
function (Heck et al., 1984; Adams et al., 1989; Lesser et al., 1990; Wang and Mauzerall, 2004; Tai et al., 2021; Feng  
et al., 2022). The selection criteria of the data are described in detail in Mills et al. (2018a).  
The yield data from the literature experiments were standardized as performed by Mills et al. (2018a) and described  
by Osborne et al. (2016). For each experiment, linear regression was used to determine the yield at 25 ppb M7 O<sub>3</sub> and  
this value was the reference for calculating the relative yield, i.e., relative yield was calculated as the actual observed  
310 yield divided by the yield at 25 ppb O<sub>3</sub>. The 25 ppb M7 O<sub>3</sub> threshold was chosen for proper comparison to the model  
results. After calculating the yield relative to 25 ppb M7 O<sub>3</sub>, a linear regression for each cultivar was performed using  
R statistical software, v4.3.0, (R Core Team, 2023; Wickham, 2016; Wickham et al., 2023) to determine the O<sub>3</sub>  
exposure response (Fig. S2). The cultivar O<sub>3</sub> exposure responses were then classified into three evenly distributed  
quantiles, 0%-33%, 33%-66%, and 66%-100%, chosen to represent the three O<sub>3</sub> sensitivity classifications: sensitive,  
315 intermediate, and tolerant, respectively (Fig. S3). These data were used to determine the model FOZ<sub>1</sub> and SFOZ<sub>1</sub>  
values of each of the O<sub>3</sub> cultivar classifications shown in Table 1 to evaluate if the models could accurately reproduce  
the O<sub>3</sub> exposure-yield responses.

### 3 Results

#### 3.1 Calibration of crop models and simulated relative yield loss against O<sub>3</sub> exposure field experiments

320 The simulated phenology (anthesis [flowering] and physiological maturity dates), biomass, yield, and relative yield  
loss due to O<sub>3</sub> stress from the maize and soybean experiments were compared to the field observations to determine  
performance of the O<sub>3</sub> equations within the models (Tables 3 – 5, Fig. 2 and 3, Fig. S1). The relative yield loss due to  
O<sub>3</sub> stress was calculated by dividing the yield of each corresponding O<sub>3</sub> treatment over the control yield, i.e., the  
baseline O<sub>3</sub> treatment. There was no O<sub>3</sub> field experiment data for rice, so the rice O<sub>3</sub> parameter values and performance  
325 were compared to the O<sub>3</sub> exposure-yield response functions from the literature (section 3.3).  
The maize and soybean cultivars had different sensitivities to O<sub>3</sub> stress which were accounted for by using different  
FOZ<sub>1</sub> and SFOZ<sub>1</sub> values (Fig. S1). The calibrated CERES-Maize and CROPGRO-Soybean models simulated the  
physiological maturity within four days of the observations (Table 5; Root Mean Square Error (RMSE) = 0.0 days for  
maize 2018, 3.70 days for soybean 2009, and 3.30 days for soybean 2010). The calibrated CERES-Maize model was  
330 able to reproduce the yield and relative yield loss very well across all six cultivars (Fig. 2; RMSE = 107 kg ha<sup>-1</sup> and  
2%; r<sup>2</sup> = 0.99 and 0.99, respectively). This ideal model performance was because only two O<sub>3</sub> treatments were  
available for each maize cultivar which simplified the calibration process (Fig. S1 (a)). The CROPGRO-Soybean  
model was able to reproduce the biomass, yield, and relative yield loss due to O<sub>3</sub> stress well for the calibration year,  
2009 (Fig. 3 (a), (b), (c); RMSE = 1179 kg ha<sup>-1</sup>, 328 kg ha<sup>-1</sup>, and 10%; r<sup>2</sup> = 0.81, 0.88, and 0.85), and acceptably for



335 the evaluation year, 2010, across all seven cultivars (Fig. 3 (d), (e), (f); RMSE = 3339 kg ha<sup>-1</sup>, 1291 kg ha<sup>-1</sup>, and 16%;  
 $r^2 = 0.59, 0.71, \text{ and } 0.66$ ). The model overestimated biomass and yield for all cultivars and treatments in 2010, which  
 was likely the result of a factor outside of the model setup that mitigated the increased incoming solar radiation when  
 compared to 2009 (section 4.3). The calibration and evaluation for the NWheat model was conducted and validated  
 in Guarin et al. (2019), where the model reproduced the observed relative yield due to O<sub>3</sub> stress with a Normalized  
 340 Root Mean Square Error (NRMSE) of 23% and an  $r^2$  of 0.94, 0.91, and 0.88 for the tolerant, intermediate, and sensitive  
 O<sub>3</sub> sensitive cultivar classifications.

345 **Table 3: CERES-Maize cultivar and O<sub>3</sub> parameters used to simulate the six maize cultivars from the 2018 FACE field  
 experiment (Choquette et al., 2020). P1 = Thermal time from seedling emergence to the end of the juvenile phase  
 (expressed in degree days above a base temperature of 8 °C), P2 = Extent to which daily development is delayed for each  
 hour increase in photoperiod above the longest photoperiod at which development proceeds at a maximum rate (which is  
 considered to be 12.5 hours), P5 = Thermal time from silking to physiological maturity (expressed in degree days above a  
 base temperature of 8 °C), G2 = Maximum possible number of kernels per plant, G3 = Kernel filling rate during the  
 linear grain filling stage and under optimum conditions (mg day<sup>-1</sup>), PHINT = Phylochron interval, i.e., the interval in  
 350 thermal time (degree days) between successive leaf tip appearances, FOZ<sub>1</sub> = O<sub>3</sub> effect on photosynthesis, and SFOZ<sub>1</sub> = O<sub>3</sub>  
 effect on leaf senescence.**

Cultivar	P1	P2	P5	G2	G3	PHINT	FOZ <sub>1</sub>	SFOZ <sub>1</sub>
B73 x Hp301	110	0.5	700	700	8.5	38.9	0.40	0.20
B73_x_Mo17	110	0.5	700	700	5.9	38.9	0.20	0.15
B73_x_NC338	110	0.5	700	700	7.8	38.9	0.65	0.40
Mo17 x Hp301	110	0.5	700	700	5.5	38.9	0.10	0.10
Mo17_x_NC338	110	0.5	700	700	8.5	38.9	0.50	0.30
NC338_x_Hp301	110	0.5	700	700	5.1	38.9	0.10	0.10



**Table 4: CROPGRO-Soybean cultivar and O<sub>3</sub> parameters used to simulate the seven soybean cultivars based on the maturity groups defined in the SoyFACE field experiment (Betzelberger et al., 2012). CSDL = Critical Short Day Length below which reproductive development progresses with no daylength effect (for shortday plants) (hour), PPSSEN = Slope of the relative response of development to photoperiod with time (positive for shortday plants) (per hour), EM-FL = Time between plant emergence and flower appearance (R1) (photothermal days), FL-SH = Time between first flower and first pod (R3) (photothermal days), FL-SD = Time between first flower and first seed (R5) (photothermal days), SD-PM = Time between first seed (R5) and physiological maturity (R7) (photothermal days), FL-LF = Time between first flower (R1) and end of leaf expansion (photothermal days), LEMAX = Maximum leaf photosynthesis rate at 30 °C, 350 ppm CO<sub>2</sub>, and high light (mg CO<sub>2</sub> m<sup>-2</sup> s<sup>-1</sup>), SLAVR = Specific leaf area of cultivar under standard growth conditions (cm<sup>2</sup> g<sup>-1</sup>), SZLF = Maximum size of full leaf (three leaflets) (cm<sup>2</sup>), XFRT = Maximum fraction of daily growth that is partitioned to seed and shell, WTPSD = Maximum weight per seed (g), SFDUR = Seed filling duration for pod cohort at standard growth conditions (photothermal days), SDPDV = Average seed per pod under standard growing conditions (number per pod), PODUR = Time required for cultivar to reach final pod load under optimal conditions (photothermal days), THRSH = Threshing percentage. The maximum ratio of (seed per (seed + shell)) at maturity, SDPRO = Fraction protein in seeds (g(protein) per g(seed)), SDLIP = Fraction oil in seeds (g(oil) per g(seed)), FOZ<sub>1</sub> = O<sub>3</sub> effect on photosynthesis, and SFOZ<sub>1</sub> = O<sub>3</sub> effect on leaf senescence.**

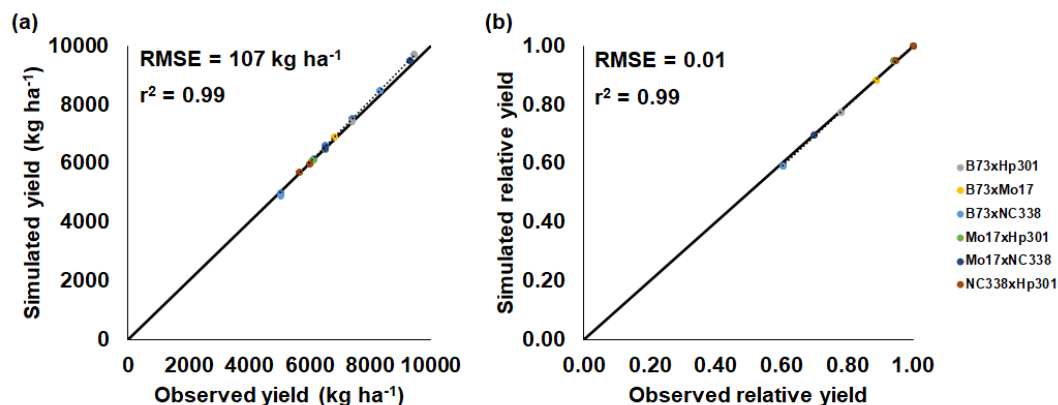
Cultivar	Maturity Group	CSDL	PPSEN	EM-FL	FL-SH	FL-SD	SD-PM	FL-LF	LEMAX	SLAVR	SZLF	XFRT	WTPSD	SFDUR	SDPDV	PODUR	THRSH	SDPRO	SDLIP	FOZ <sub>1</sub>	SFOZ <sub>1</sub>
Pioneer 93B15	3	13.1	0.285	19.0	6	14.0	33.2	26	1.20	375	180	1	0.16	23	2.2	10	77	0.405	0.205	0.25	0.25
Dwight	2	12.9	0.249	17.4	6	13.5	32.4	26	1.00	375	180	1	0.16	23	2.2	10	77	0.405	0.205	0.20	0.20
HS93-4118	4	13.3	0.294	19.4	7	15.0	34.0	26	1.05	375	180	1	0.16	23	2.2	10	77	0.405	0.205	0.30	0.30
IA-3010	3	13.2	0.285	19.0	6	14.0	33.2	26	1.01	375	180	1	0.16	23	2.2	10	77	0.405	0.205	0.25	0.25
LN97-15076	4	13.2	0.294	19.4	7	15.0	34.0	26	1.08	375	180	1	0.19	23	2.2	10	77	0.405	0.205	0.30	0.30
Loda	2	12.7	0.249	17.4	6	13.5	32.4	26	1.03	375	180	1	0.19	23	2.2	10	77	0.405	0.205	0.30	0.30
Pana	3	13.0	0.285	19.0	6	14.0	33.2	26	1.00	375	180	1	0.15	23	2.2	10	77	0.405	0.205	0.25	0.25



355 **Table 5: Observed and simulated anthesis day and maturity day for the six maize cultivars from the 2018 FACE experiment (Choquette et al., 2020) and the seven soybean cultivars from the 2009 and 2010 soybean SoyFACE experiments (Betzelberger et al., 2012). The observed maturity dates were estimated from the single reported harvest date for all cultivars but there may have been minor variation between the different cultivars. Observed anthesis was not available for soybean.**

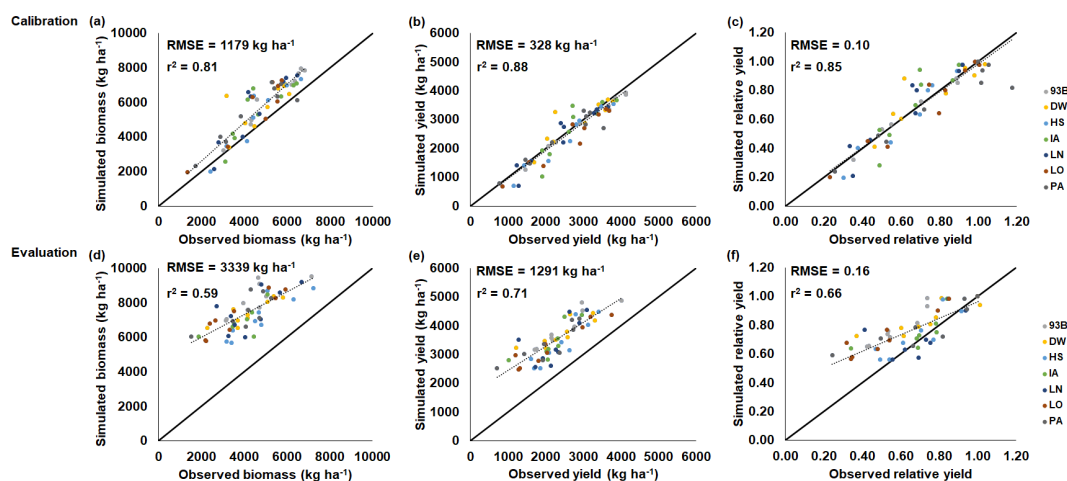
Crop experiment	Cultivar	Observed anthesis (dap)	Simulated anthesis (dap)	Observed maturity (dap)	Simulated maturity (dap)
Maize 2018	B73 x Hp301	48	48	97	97
	B73 x Mo17	48	48	97	97
	B73_x_NC338	48	48	97	97
	Mo17 x Hp301	48	48	97	97
	Mo17 x NC338	48	48	97	97
	NC338 x Hp301	48	48	97	97
Soybean 2009	Pioneer93B15		52	133	131
	Dwight		48	133	126
	HS93-4118		53	133	133
	IA-3010		50	133	128
	LN97-15076		55	133	137
	Loda		52	133	132
	Pana		54	133	134
Soybean 2010	Pioneer93B15		48	126	129
	Dwight		44	126	125
	HS93-4118		48	126	129
	IA-3010		47	126	126
	LN97-15076		50	126	131
	Loda		48	126	130
	Pana		51	126	131

360



365

**Figure 2: CERES-Maize model calibration of the 2018 FACE O<sub>3</sub> field experiment conducted in Champaign, Illinois, USA (Choquette et al., 2020). Simulated and observed (a) yield and (b) relative yield loss due to elevated O<sub>3</sub> stress (compared to the ambient control treatment) for six maize cultivars (colored points). The root-mean-square error (RMSE) and coefficient of determination (r<sup>2</sup>) show the model performance across all cultivars. Solid black line shows 1:1 comparison and dotted black line shows linear fit across all cultivars. For maize only one year of experimental data was available for calibration and evaluation. The model cultivar parameters are shown in Table 3.**

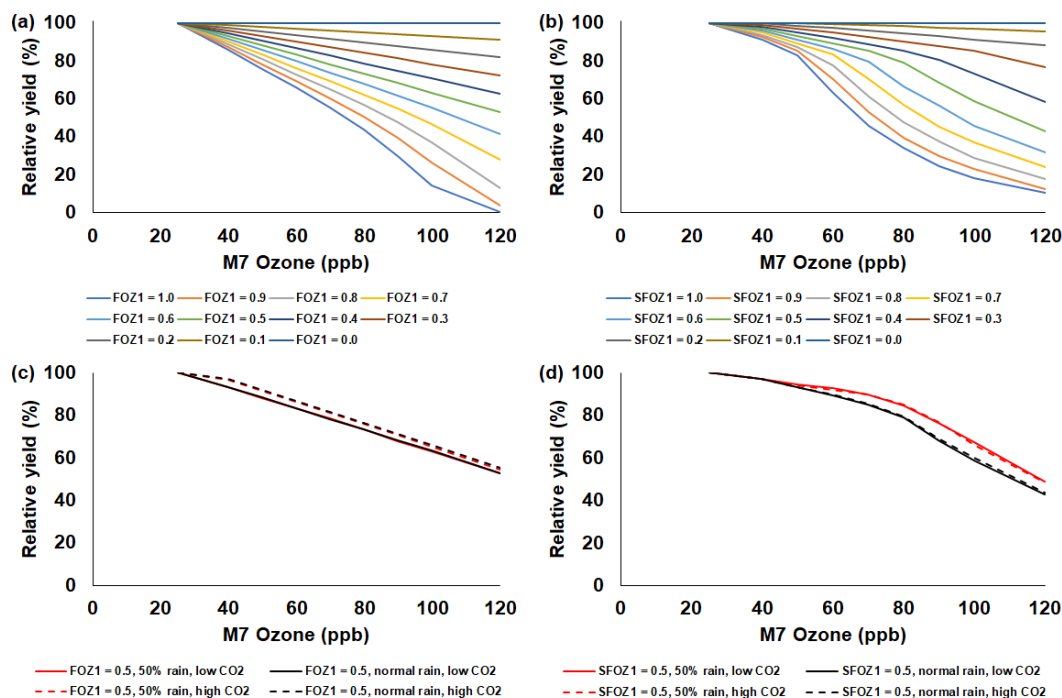


370 **Figure 3: CROPGRO-Soybean model performance and evaluation of the SoyFACE O<sub>3</sub> field experiment conducted in**  
**Champaign, Illinois, USA (Betzberger et al., 2012). Simulated and observed (a, d) above-ground biomass, (b, e) yield,**  
**and (c, f) relative yield loss in response to the nine progressive O<sub>3</sub> increasing treatments (Table 2) for seven soybean**  
**cultivars (colored points). Relative yield loss is compared to the ambient control treatment within each year. The 2009**  
**SoyFACE field experiment was used for model calibration (a, b, c), and the 2010 SoyFACE field experiment was used for**  
**model evaluation (d, e, f). The root-mean-square error (RMSE) and coefficient of determination (r<sup>2</sup>) show the model**  
375 **performance across all cultivars. Solid black line shows 1:1 comparison and dotted black line shows linear fit across all**  
**cultivars. The model cultivar parameters are shown in Table 4.**

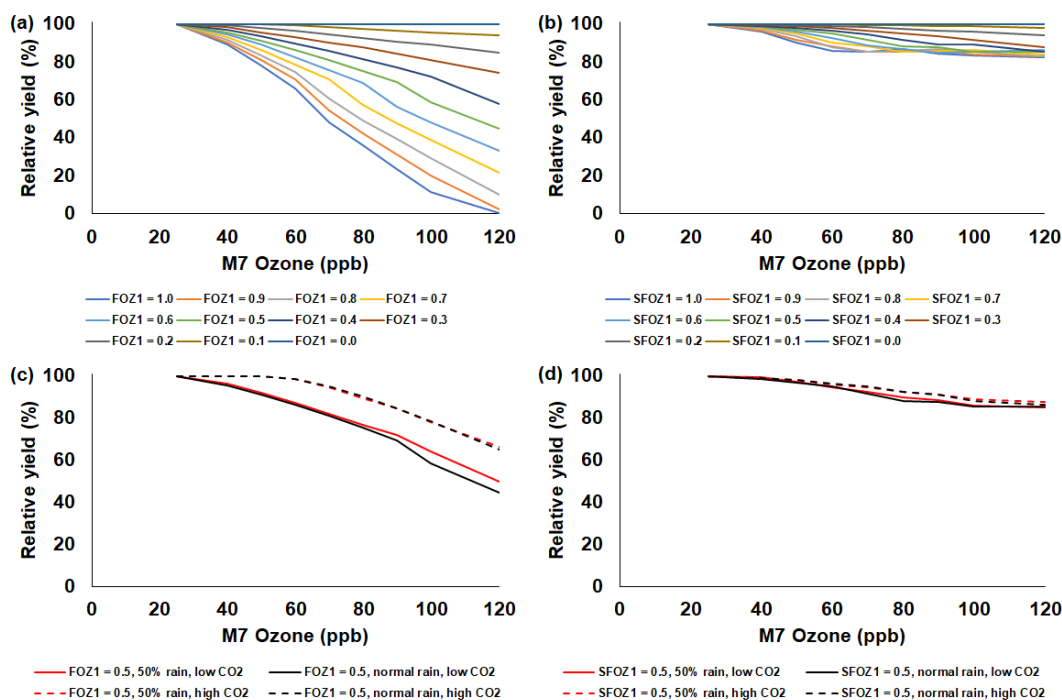
### 3.2 Sensitivity analysis and combined effects of O<sub>3</sub>, CO<sub>2</sub>, and water deficit stress on yields

The simulated relative yield losses due to O<sub>3</sub> stress increased for all crops as the M7 O<sub>3</sub> concentrations increased above the 25 ppb threshold when examining the photosynthesis and leaf senescence responses independently, as expected  
380 (Figs. 4 – 7). The simulated actual yields for all crops are shown in the Supplementary Tables S2 – S9. Wheat was the most sensitive crop to O<sub>3</sub> stress of the four crops examined (compare slopes in Figs. 4 – 7 (a) and (b)) which agrees with previous literature (Mills et al., 2018a). For each model, simulations using a FOZ<sub>1</sub> or SFOZ<sub>1</sub> example value of 0.5 were examined in more detail to illustrate the O<sub>3</sub>-CO<sub>2</sub>-water interactions (Figs. 4 – 7 (c) and (d), respectively). For all crops, the Dry/reduced rainfall and low CO<sub>2</sub> treatment produced the lowest yields while the Wet/normal rainfall  
385 and high CO<sub>2</sub> produced the highest yields (Tables S2 – S9). The simulated O<sub>3</sub> effect was larger when water deficit stress was non-limiting, i.e., the higher rainfall and irrigated treatments experienced larger losses due to O<sub>3</sub> stress because of increased stomatal uptake. The simulated O<sub>3</sub> effect was reduced under the higher CO<sub>2</sub> concentrations, thus capturing the responses from stomatal closure and the photosynthetic benefits from the CO<sub>2</sub> fertilization effect.

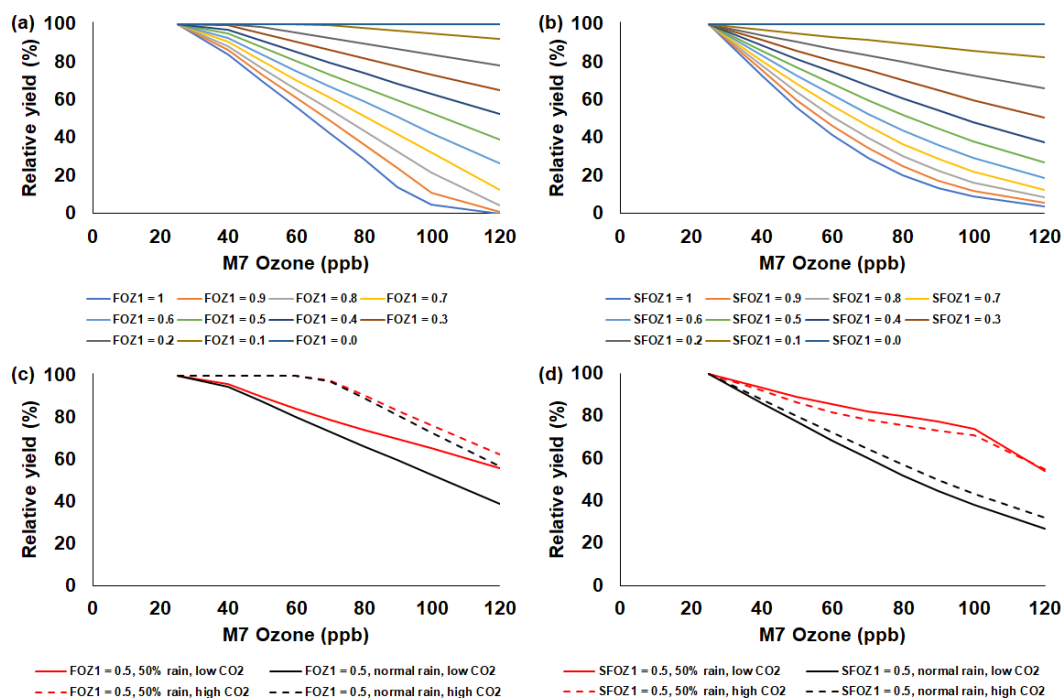




390 Figure 4: Sensitivity analysis using the CERES-Maize model to simulate O<sub>3</sub> relative yield loss for a range of (a) the  
 photosynthesis O<sub>3</sub> stress parameter (FOZ<sub>1</sub>) and (b) the leaf senescence O<sub>3</sub> stress parameter (SFOZ<sub>1</sub>) values under the  
 normal rainfall and 350 ppm CO<sub>2</sub> scenario, and an example of (c) FOZ<sub>1</sub> and (d) SFOZ<sub>1</sub> set at 0.5 under the 50% reduced  
 395 rainfall and 350 ppm CO<sub>2</sub> (solid red line), normal rainfall and 350 ppm CO<sub>2</sub> (solid black line), 50% less rainfall and 550  
 ppm CO<sub>2</sub> (dashed red line), and normal rainfall and 550 CO<sub>2</sub> (dashed black line) scenarios. The Champaign, Illinois, USA  
 2018 FACE weather, soil, and dominant management conditions were used for the reference location. Each O<sub>3</sub> parameter  
 was tested independently, i.e., when examining FOZ<sub>1</sub>, SFOZ<sub>1</sub> was set to zero and vice versa. The simulated actual yields  
 are shown in Tables S2 and S3.

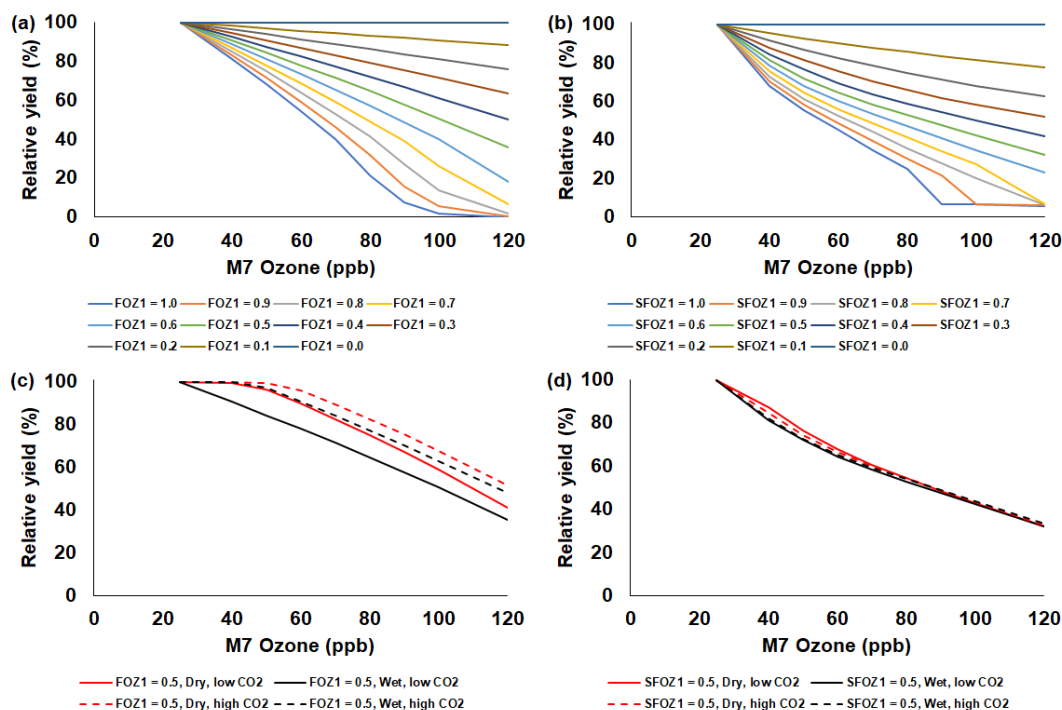


400 **Figure 5: Sensitivity analysis using the CERES-Rice model to simulate O<sub>3</sub> relative yield loss for a range of (a) FOZ<sub>1</sub> and**  
**(b) SFOZ<sub>1</sub> values under the normal rainfall and 350 ppm CO<sub>2</sub> scenario, and an example of (c) FOZ<sub>1</sub> and (d) SFOZ<sub>1</sub> set at**  
**0.5 under the 50% reduced rainfall and 350 ppm CO<sub>2</sub> (solid red line), normal rainfall and 350 ppm CO<sub>2</sub> (solid black line),**  
**50% less rainfall and 550 ppm CO<sub>2</sub> (dashed red line), and normal rainfall and 550 CO<sub>2</sub> (dashed black line) scenarios. The**  
**Stuttgart, Arkansas, USA 2009 weather, soil, and dominant management conditions were used for the reference location.**  
 Each O<sub>3</sub> parameter was tested independently, i.e., when examining FOZ<sub>1</sub>, SFOZ<sub>1</sub> was set to zero and vice versa. The  
 405 simulated actual yields are shown in Tables S4 and S5.



410

**Figure 6:** Sensitivity analysis using the CROPGRO-Soybean model to simulate  $O_3$  relative yield loss for a range of (a)  $FOZ_1$  and (b)  $SFOZ_1$  values under the normal rainfall and 350 ppm  $CO_2$  scenario, and an example of (c)  $FOZ_1$  and (d)  $SFOZ_1$  set at 0.5 under the 50% reduced rainfall and 350 ppm  $CO_2$  (solid red line), normal rainfall and 350 ppm  $CO_2$  (solid black line), 50% less rainfall and 550 ppm  $CO_2$  (dashed red line), and normal rainfall and 550  $CO_2$  (dashed black line) scenarios. The Champaign, Illinois, USA 2009 SoyFACE weather, soil, and dominant management conditions were used for the reference location. Each  $O_3$  parameter was tested independently, i.e., when examining  $FOZ_1$ ,  $SFOZ_1$  was set to zero and vice versa. The simulated actual yields are shown in Tables S6 and S7. Figure S6 shows the relative biomass loss corresponding to  $SFOZ_1$  (d) to explain the inverted  $CO_2$  effect under the 50% rainfall treatment.



415

420

Figure 7: Sensitivity analysis using the NWheat model to simulate O<sub>3</sub> relative yield loss for a range of (a) FOZ<sub>1</sub> and (b) SFOZ<sub>1</sub> values under the “Wet” irrigation and 350 ppm CO<sub>2</sub> scenario, and an example of (c) FOZ<sub>1</sub> and (d) SFOZ<sub>1</sub> set at 0.5 under the “Dry” irrigation and 350 ppm CO<sub>2</sub> (solid red line), “Wet” irrigation and 350 ppm CO<sub>2</sub> (solid black line), “Dry” irrigation and 550 ppm CO<sub>2</sub> (dashed red line), and “Wet” irrigation and 550 ppm CO<sub>2</sub> (dashed black line) scenarios. The Maricopa, Arizona, USA 1993 FACE weather, soil, and management conditions were used for the reference location (Kimball et al., 1999; Guarin et al., 2019). Each O<sub>3</sub> parameter was tested independently, i.e., when examining FOZ<sub>1</sub>, SFOZ<sub>1</sub> was set to zero and vice versa. The simulated actual yields are shown in Tables S8 and S9.

### 3.3 Simulated relative yield loss compared to O<sub>3</sub> relationships in the literature

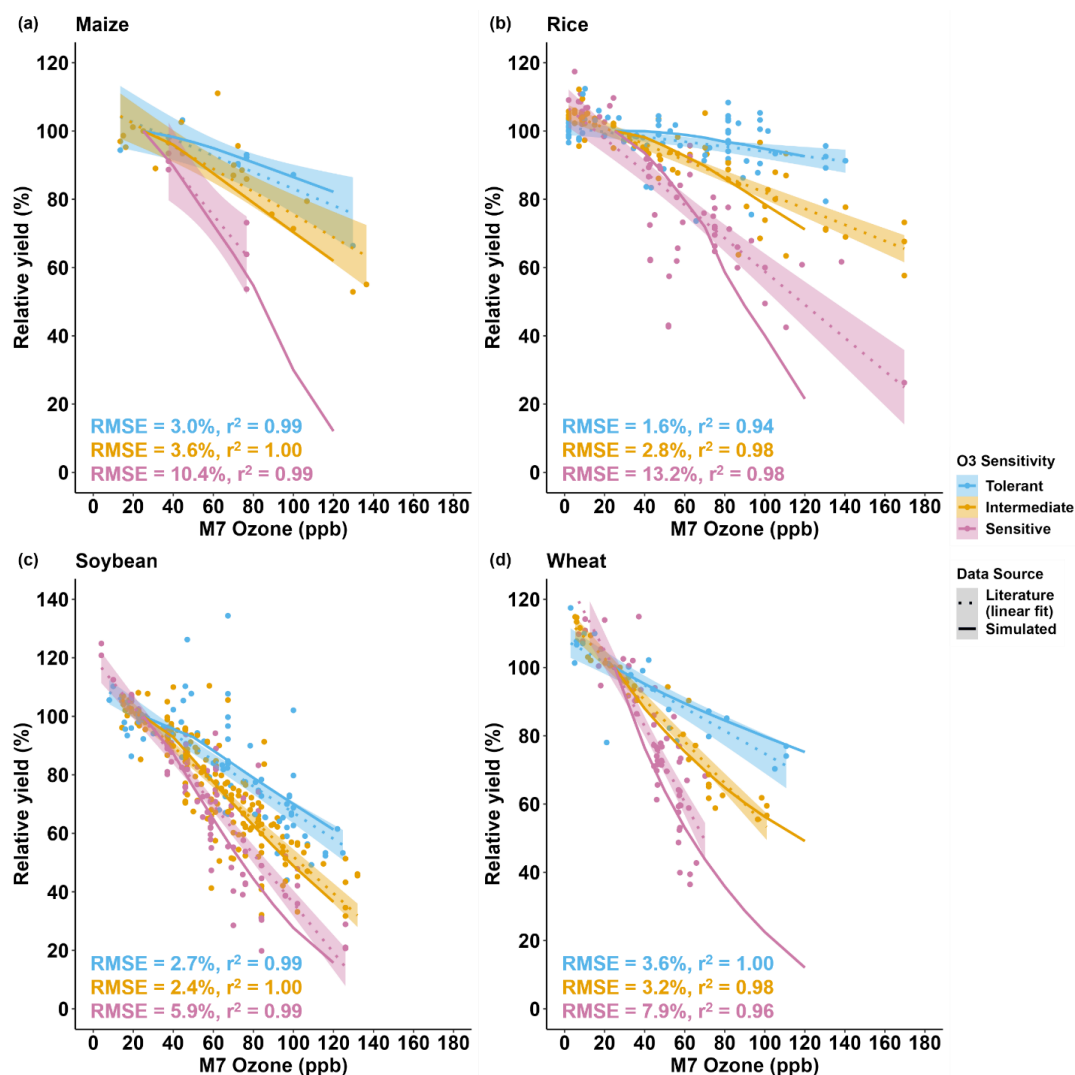
425

For all crops, the literature showed a large range of relative yield losses due to O<sub>3</sub> stress caused by different cultivar O<sub>3</sub> sensitivities (Fig. S2). Wheat was the most sensitive crop to O<sub>3</sub> stress with an average yield loss of 0.70% ± 0.39 (mean ± SD) per ppb M7 O<sub>3</sub> increase above 25 ppb, followed by soybean, maize, and then rice (average yield losses of 0.60% ± 0.39, 0.39% ± 0.26, and 0.32% ± 0.37 per ppb M7 O<sub>3</sub> increase above 25 ppb, respectively) (average of slopes in Table S10). To encompass the high variability of yield losses, the cultivars were classified into the O<sub>3</sub> tolerant, intermediate, and sensitive cultivar O<sub>3</sub> sensitivities (Fig. S3). Since the cultivar sensitivities were not originally specified in the literature, the FOZ<sub>1</sub> and SFOZ<sub>1</sub> parameters used in the models were adjusted to provide the best fit across the O<sub>3</sub> exposure responses (Table 1). Overall, the models reproduced the simulated O<sub>3</sub> exposure relationships from the literature well; the RMSE for maize, rice, soybean, and wheat across all three O<sub>3</sub> exposure sensitivities were 6.6%, 7.8%, 4.0%, and 5.4%, respectively (Fig. 8). The models performed better (lower RMSE) for the O<sub>3</sub> tolerant and O<sub>3</sub> intermediate cultivar sensitivities compared to the O<sub>3</sub> sensitive cultivar sensitivity, but all

435



models explained the variance well ( $r^2 > 0.96$  across all O<sub>3</sub> sensitivities). This suggests that different combinations of FOZ<sub>1</sub> and SFOZ<sub>1</sub> can be calibrated for specific observations to emulate the variation in different O<sub>3</sub> exposure responses.



440

445

Figure 8: Simulated relative yield loss due to O<sub>3</sub> stress (solid lines) compared to the O<sub>3</sub> exposure relationships (dotted lines) from the literature data (symbols) for the (a) CERES-Maize, (b) CERES-Rice, (c) CROPGRO-Soybean, and (d) NWheat models. The O<sub>3</sub> exposure-yield response linear functions of the three O<sub>3</sub> sensitivities: tolerant (blue), intermediate (gold), and sensitive (magenta) are given in Figure S3. The cultivars were classified by grouping the cultivar O<sub>3</sub> exposure-yield response (Fig. S2) into three evenly distributed quantiles: 66%-100%, 33%-66%, and 0%-33%, respectively. The O<sub>3</sub> sensitivities determined for each cultivar are listed in Table S10. The simulated results for the crop models use the FOZ<sub>1</sub> and SFOZ<sub>1</sub> values from Table 1. For each model, the same weather, soil, and dominant management conditions as in the normal rainfall and 350 ppm CO<sub>2</sub> treatment of the sensitivity analysis were used as reference (the O<sub>3</sub> response functions from the literature included O<sub>3</sub> field experiments conducted when the atmospheric CO<sub>2</sub> concentration



450 was ~350 ppm). The literature data consists of the relative yields (scaled to 25 ppb M7 O<sub>3</sub>) of the cultivars examined in the  
Mills et al. (2018a) literature review combined with the maize and soybean cultivars used in this study for a total of 9  
maize cultivars, 50 rice cultivars, 49 soybean cultivars, and 23 wheat cultivars (listed in Table S10). For the O<sub>3</sub> sensitivity  
of each crop, the root-mean-square error (RMSE) and coefficient of determination ( $r^2$ ) show the model performance  
455 compared to the linear fit of the O<sub>3</sub> exposure literature data (text color corresponds to O<sub>3</sub> sensitivity). The color shaded  
area shows the standard error for the linear fit of the literature data for each of the cultivar O<sub>3</sub> sensitivities.

## 4 Discussion

### 4.1 Simulating O<sub>3</sub> damage on crop yields

The measured yield losses for the maize FACE experiment were between 5% to 40% for the M7 O<sub>3</sub> concentrations  
when increasing from the ambient concentration (38 ppb) to the elevated O<sub>3</sub> treatment (77 ppb), a yield loss of 0.14%  
460 to 1.01% per ppb M7 O<sub>3</sub> above the ambient concentration, depending on the O<sub>3</sub> cultivar sensitivity (Fig. 2b). Cv.  
NC338xHp301 and cv. Mo17xHp301 were classified as O<sub>3</sub> tolerant because of relatively small yield losses of 5% and  
6%, respectively; cv. B73xMo17 was classified as O<sub>3</sub> intermediate with a yield loss of 11%; and cv. B73xHp301, cv.  
Mo17xNC338, and cv. B73xNC338 were sensitive to O<sub>3</sub> effects with yield losses of 22%, 30%, and 40%, respectively  
(Fig. S1a, Table S10). These cultivar O<sub>3</sub> sensitivities are based on a single experimental year so additional testing is  
465 needed to further corroborate the classifications. Overall, the calibrated CERES-Maize model was able to reproduce  
these observed yield losses within 1%, i.e., simulated yield losses between 5% to 41%, or 0.12% to 1.05% per ppb O<sub>3</sub>  
increase above the ambient concentration. These yield losses were also calculated relative to 25 ppb (as described in  
section 2.5) for consistency with the literature, which resulted in simulated yield losses between 0.12% to 0.93% per  
ppb M7 O<sub>3</sub> increase above 25 ppb across the six cultivars.

470 When comparing the simulations to the maize O<sub>3</sub> exposure-yield relationships from the literature, the model simulated  
average yield losses of 0.16%, 0.36%, and 0.82% per ppb M7 O<sub>3</sub> increase above 25 ppb for the O<sub>3</sub> tolerant,  
intermediate, and sensitive cultivar O<sub>3</sub> sensitivities, respectively (Fig. 8 (a) solid lines). This agreed well with the  
literature yield losses of 0.24%, 0.33%, and 0.71% per ppb M7 O<sub>3</sub> increase above 25 ppb for the O<sub>3</sub> tolerant,  
intermediate, and sensitive cultivar sensitivities, respectively (Fig. S3 (a), Fig. 8 (a) dotted lines). The O<sub>3</sub> parameter  
475 values used for the literature comparison were determined to provide the best fit across the literature experiments  
consisting of nine maize cultivars, but these O<sub>3</sub> parameter values could be calibrated for other scenarios and cases,  
i.e., higher or lower cultivar O<sub>3</sub> sensitivity.

The measured yield losses for the SoyFACE experiment were between 51% to 77% for the M7 O<sub>3</sub> concentrations  
when increasing from the ambient concentration (37 ppb) to the highest O<sub>3</sub> treatment (126 ppb) in 2009, a yield loss  
480 of 0.57% to 0.86% per ppb M7 O<sub>3</sub> above the ambient concentration, depending on the cultivar O<sub>3</sub> sensitivity (Fig. 3  
(c)). The calibrated CROPGRO-Soybean model reproduced observed yields losses within 10%, i.e., simulated yield  
losses between 59% to 80%, or 0.66% to 0.90% per ppb O<sub>3</sub> increase. Based on the calculated O<sub>3</sub> classifications from  
the literature and low yield divergence across the seven cultivars (Fig. S1 (b)), cv. Pioneer93B15, cv. Dwight, cv. IA-  
3010, and LN97-15076 were considered O<sub>3</sub> intermediate sensitivity, and cv. HS93-4118, cv. Loda, and cv. Pana were  
485 considered O<sub>3</sub> sensitive (Table S10). In 2010, the observed soybean yield losses ranged between 31% to 76% when  
increasing from the ambient concentration (37 ppb) to the highest O<sub>3</sub> treatment (84 ppb), a yield loss of 0.65% to  
1.60% per ppb M7 O<sub>3</sub> above the ambient concentration. The model underestimated yield losses in 2010, between 27%



to 44%, but because the experimental setup was the same for both years, an external factor may have affected yields that was not considered in the simulations (section 4.3). The 2010 yield losses were a similar magnitude to the 2009  
490 yield losses, but the 2010 experiment had higher yield loss and variation per ppb O<sub>3</sub> increase with lower average M7 O<sub>3</sub> concentrations (Table 2, Fig. S4 (a)).

When comparing the simulations to the soybean O<sub>3</sub> exposure-yield relationships from the literature (Fig. 8 (c)), an average yield loss of 0.36%, 0.64%, and 0.96% per ppb M7 O<sub>3</sub> increase above 25 ppb was simulated for the O<sub>3</sub> tolerant, intermediate, and sensitive cultivar O<sub>3</sub> sensitivities, respectively. This was substantiated by the literature yield losses  
495 of 0.45%, 0.63%, and 0.84% per ppb M7 O<sub>3</sub> increase above 25 ppb for the O<sub>3</sub> tolerant, intermediate, and sensitive cultivar O<sub>3</sub> sensitivities, respectively (Fig. S3 (c), Fig. 8 (c) dotted lines). The literature data consisted of 49 soybean cultivars, which had a smaller range of O<sub>3</sub> sensitivities compared to the other crops, although there were outliers where yield increased under higher O<sub>3</sub> concentrations (described in section 4.2).

The CERES-Rice model simulated an average yield loss of 0.05%, 0.23%, and 0.66% per ppb M7 O<sub>3</sub> increase above  
500 25 ppb for the O<sub>3</sub> tolerant, intermediate, and sensitive cultivar O<sub>3</sub> sensitivities, respectively (Fig. 8 (b) solid lines). The rice literature had the most cultivars (50) of the four crops examined, and the simulated yield losses for the O<sub>3</sub> tolerant and intermediate cultivar O<sub>3</sub> sensitivities agreed well with the literature yield losses of 0.07% and 0.24% per ppb M7 O<sub>3</sub> increase above 25 ppb, respectively (Fig. 8 (b) dotted lines). A larger discrepancy between the simulated yield loss for the O<sub>3</sub> sensitive classification and the literature O<sub>3</sub> sensitive yield loss of 0.49% per ppb M7 O<sub>3</sub> increase above 25  
505 ppb was due to the higher variability within the literature data (Fig. 8 (b) shaded area).

Using the calibrated NWheat model, the simulated yield losses were 0.26%, 0.66%, and 1.23% per ppb M7 O<sub>3</sub> increase above 25 ppb for the O<sub>3</sub> tolerant, intermediate, and sensitive cultivar O<sub>3</sub> sensitivities, respectively (Fig 8 (d)). These simulated yield losses were corroborated by the reported average yield losses of 0.33%, 0.61%, and 1.11% per ppb M7 O<sub>3</sub> increase above 25 ppb for the O<sub>3</sub> tolerant, intermediate, and sensitive cultivar O<sub>3</sub> sensitivities, respectively.  
510 The literature expanded across different ranges of O<sub>3</sub> concentrations for all crops, and yield loss per ppb is not always constant over an expansive range of O<sub>3</sub> concentrations, so the model O<sub>3</sub> parameter values can be adjusted for higher or lower cultivar O<sub>3</sub> sensitivity.

#### 4.2 Simulated relative yield loss with the combined effects of O<sub>3</sub>, CO<sub>2</sub>, and water deficit stress

The sensitivity analyses showed that the yield losses due to O<sub>3</sub> stress were higher under the normal rainfall and low  
515 CO<sub>2</sub> treatment which agrees with previous literature that increased water availability increases O<sub>3</sub> impact due to increased stomatal uptake (Khan and Soja, 2003; Biswas et al., 2013). It was unexpected that the simulated O<sub>3</sub> photosynthetic response difference between the normal and reduced rainfall treatments for maize was less than 1% (Fig. 4 (c)). This was because the model simulated low water deficit stress under the 50% reduced rainfall treatment which obscured the O<sub>3</sub>-water stress dynamics. Further reducing the rainfall to 40% of the normal amount increased  
520 the simulated water deficit stress and produced the photosynthetic O<sub>3</sub>-water dynamics consistent with the other models (Fig. S5). The elevated CO<sub>2</sub> concentration mitigated the detrimental effect of O<sub>3</sub> stress in the photosynthetic response for all models (Figs. 4 – 7 (c)), which agrees with recent global findings that elevated CO<sub>2</sub> concentrations can mitigate and even negate elevated O<sub>3</sub> impacts (Xia et al., 2021; Tai et al., 2021). Interestingly, the CROPGRO-Soybean model





525 simulated an inverse O<sub>3</sub>-CO<sub>2</sub> effect on relative yield under the 50% rainfall condition when examining SFOZ<sub>1</sub> in detail (Fig. 6 (d)). This inverse yield response was due to the low actual yield simulated under the 50% rainfall and low CO<sub>2</sub> treatment (< 2,000 kg ha<sup>-1</sup>, Table S7) which resulted in smaller changes in yield compared to the 50% rainfall and high CO<sub>2</sub> treatment, but the overall simulated aboveground biomass O<sub>3</sub>-CO<sub>2</sub>-water interaction was as expected (Fig. S6).

530 For several of the observations from the actual soybean field experiment using cv. Pana, the yield increased under higher O<sub>3</sub> concentrations (~2% to 18%, Fig. 3 (c) and Fig. S1 (b)). In some cases it is possible that elevated O<sub>3</sub> concentrations can benefit a crop via hormesis, a process where low levels of intermittent stress may benefit overall crop growth through improved resiliency (Calabrese, 2014). It is also possible that if elevated O<sub>3</sub> concentrations reduce biomass growth throughout the season, and therefore reduce nutrient resource demand throughout the season, small yield increases can occur from a larger pool of resources available during the key reproductive/grain filling period  
535 (Asseng and Van Herwaarden, 2003; Guarin et al., 2019). This increase in yield under higher O<sub>3</sub> concentrations was also observed under several other soybean and rice cultivars from the literature (Fig. S2 (b) and (c)). However, a soybean cultivar from the literature, cv. Cumberland, was reported to have a 34% increase under elevated O<sub>3</sub> (67 ppb) compared to the control treatment (25 ppb), but such a large increase may indicate that another outside factor affected the yields.

#### 540 **4.3 Uncertainty in model simulations and O<sub>3</sub> exposure field experiments**

Crop models contain uncertainties due to simplification of complex biological processes, but field experiments may also contribute uncertainty via measurement. The soybean simulations overestimated both biomass and yield across all cultivars and treatments for the 2010 SoyFACE experiment. Since both the ambient and elevated O<sub>3</sub> treatments were overestimated, it is unlikely that the simulated O<sub>3</sub> interactions caused the discrepancy. Examining the weather  
545 input showed a 14% increase in cumulative incoming solar radiation for the 2010 growing season compared to the 2009 growing season (Fig. S4 (b)). The 2010 season was warmer than the 2009 season, average seasonal temperature of 23.4 °C compared to 19.1 °C, but no heat stress was reported and the difference in rainfall was negligible, 445 mm compared to 454 mm. Since management was the same for both years and no water or N stresses were reported, it was expected that the 2010 yields would be higher than the 2009 yields due to the increased solar radiation, but the average  
550 2010 yield across all cultivars for the ambient treatment decreased, 3300 kg ha<sup>-1</sup> in 2010 compared to 3700 kg ha<sup>-1</sup> in 2009. Therefore, it is possible that an outside stress factor not considered within the model limited soybean growth in the field in 2010 which led to the model overestimating biomass and yield.

The sensitivity analyses showed that the CO<sub>2</sub> effect was more pronounced in the model photosynthesis response than in the leaf senescence response (compare solid and dashed lines in Figs. 4 – 7 (c) and (d)). This is because the models  
555 do not have a CO<sub>2</sub> effect directly applied to the daily leaf senescence calculation, whereas CO<sub>2</sub> directly affects the daily photosynthesis calculation (PCARB in Eq. (3) and (4), and PRATIO in Eq. (9)). Improved CO<sub>2</sub> representation within the crop models is being explored through the Agricultural Model Intercomparison and Improvement Project (AgMIP) studies (Ahmed et al., 2017; Ahmed et al., 2019; Toreti et al., 2020), but additional high-quality data is needed for model testing.



## 560 5 Conclusion

Crop responses to elevated O<sub>3</sub> concentrations were incorporated into the DSSAT CERES-Maize, CERES-Rice, CROPGRO-Soybean, and NWheat crop models via functions reducing photosynthetic activity and accelerating leaf senescence. Model testing showed that each of the four models reproduced the observed O<sub>3</sub> response from field experiments and previous literature, as well as the expected interactions between O<sub>3</sub>, CO<sub>2</sub>, and water deficit stress.

565 This incorporation allows for improved simulation of the heterogeneity of O<sub>3</sub> impacts across geographical regions and systems, as well as across years within seasons, which is more representative of real-world interactions than using a generic damage coefficient. Overall, increasing M7 O<sub>3</sub> concentrations had a negative effect on growth and yield across all four crops, and this negative effect was exacerbated by increased water availability and ameliorated by elevated CO<sub>2</sub> concentrations. The O<sub>3</sub> impact and stress response of the crop depends on the stress severity, duration, frequency,

570 cultivar sensitivity, and seasonal timing (i.e., developmental stage) which can be accounted for by using the updated crop models.

The addition of O<sub>3</sub> stress functionality into crop models will improve simulations of global environmental interactions using a key factor that is often not included in agricultural and climate change assessments. The DSSAT models in this study can be used to simulate the O<sub>3</sub> impacts on crops in combination with climate change. To further improve

575 model performance, the models should continue to be tested with additional experimental data and compared with other O<sub>3</sub>-modified crop models as part of multi-model ensemble assessments conducted by the AgMIP (<https://agmip.org/>). The framework described here can be used by other process-based crop models, local or gridded, to incorporate O<sub>3</sub> stress interactions into the model. This model improvement also suggests potential future collaboration between crop modelers and remote sensing experts using weather and climate models with dynamic chemistry components, such as the NASA Atmosphere Observing System (<https://aos.gsfc.nasa.gov/>).

580

### Code availability

The current version of the DSSAT crop modeling platform is available to download from the DSSAT Foundation website (<https://dssat.net/>). The current version of the pSIMS framework is available to download from the RDCEP website (<http://www.rdcep.org/research-projects/psims>). The O<sub>3</sub>-modified version of the DSSAT crop models will be

585 available with the next DSSAT version release, and the O<sub>3</sub>-modified version of the pDSSAT crop models is available from the GitHub repository at [https://github.com/jguarin4/dssat-csm-os/tree/develop\\_v4.8\\_pdssat](https://github.com/jguarin4/dssat-csm-os/tree/develop_v4.8_pdssat). An archived version of the code is also available on Zenodo at <https://zenodo.org/badge/latest/doi/232137043>. The R code used to classify the cultivar O<sub>3</sub> sensitivities is available on the Harvard Dataverse at <https://doi.org/10.7910/DVN/0NN9MH>.

### Data availability

590 All field experimental and literature data used in this study are available from the sources referenced. The crop model simulated output data is available on the Harvard Dataverse at <https://doi.org/10.7910/DVN/0NN9MH>.



### Author Contribution

J.R.G. and J.J. designed and conducted the study. E.A.A. provided the O<sub>3</sub> exposure field data. K.S. collated the O<sub>3</sub> exposure literature data. J.R.G. and F.O. incorporated the O<sub>3</sub> modifications into the DSSAT/pDSSAT model code.  
595 S.A., K.B., L.E., G.H., and A.C.R. provided insight on O<sub>3</sub>-crop interactions within the crop models. J.E., I.F., and D.K. provided technical support and guidance for the pSIMS/pDSSAT framework. J.R.G. and J.J. co-wrote the manuscript. All authors contributed to editing the manuscript.

### Competing interests

The authors declare that they have no conflict of interest.

### 600 Acknowledgements

The authors would like to thank Amy Betzelberger and Nicole Choquette for sharing the O<sub>3</sub> field experiment data. J.R.G. and K.S. would like to thank Stephanie Osborne for help with collecting the O<sub>3</sub> exposure literature data. J.R.G. and J.J. were supported by the Open Philanthropy Project. J.R.G., J.J. and A.C.R. contributions were also enabled by NASA Earth Science Division support of the NASA GISS Climate Impacts Group.

### 605 References

- Adams, R. M., Glycer, J. D., Johnson, S. L., and McCarl, B. A.: A reassessment of the economic effects of ozone on United States agriculture, *Japca-the Journal of the Air & Waste Management Association*, 39, 960-968, 10.1080/08940630.1989.10466583, 1989.
- 610 Ahmed, M., Stockle, C. O., Nelson, R., and Higgins, S.: Assessment of Climate Change and Atmospheric CO<sub>2</sub> Impact on Winter Wheat in the Pacific Northwest Using a Multimodel Ensemble, *Frontiers in Ecology and Evolution*, 5, 10.3389/fevo.2017.00051, 2017.
- Ahmed, M., Stockle, C. O., Nelson, R., Higgins, S., Ahmad, S., and Raza, M. A.: Novel multimodel ensemble approach to evaluate the sole effect of elevated CO<sub>2</sub> on winter wheat productivity, *Scientific Reports*, 9, 10.1038/s41598-019-44251-x, 2019.
- 615 Ainsworth, E. A.: Understanding and improving global crop response to ozone pollution, *Plant Journal*, 90, 886-897, 10.1111/tpj.13298, 2017.
- Arias, P. A., Bellouin, N., Coppola, E., Jones, R. G., Krinner, G., Marotzke, J., Naik, V., Palmer, M. D., Plattner, G.-K., Rogelj, J., Rojas, M., Sillmann, J., Storelvmo, T., Thorne, P. W., Trewin, B., Achuta Rao, K., Adhikary, B., Allan, R. P., Armour, K., Bala, G., Barimalala, R., Berger, S., Canadell, J. G., Cassou, C., Cherchi, A., Collins, W., Collins, W. D., Connors, S. L., Corti, S., Cruz, F., Dentener, F. J., Dereczynski, C., Di Luca, A., Diongue Niang, A., Doblas-Reyes, F. J., Dosio, A., Douville, H., Engelbrecht, F., Eyring, V., Fischer, E., Forster, P., Fox-Kemper, B., Fuglestvedt, J. S., Fyfe, J. C., Gillett, N. P., Goldfarb, L., Gorodetskaya, I., Gutierrez, J. M., Hamdi, R., Hawkins, E., Hewitt, H. T., Hope, P., Islam, A. S., Jones, C., Kaufman, D. S., Kopp, R. E., Kosaka, Y., Kossin, J., Krakovska, S., Lee, J.-Y., Li, J., Mauritsen, T., Maycock, T. K., Meinshausen, M., Min, S.-K., Monteiro, P. M. S., Ngo-Duc, T., Otto, F., Pinto, I., Pirani, A., Raghavan, K., Ranasinghe, R., Ruane, A. C., Ruiz, L., Sallée, J.-B., Samsat, B. H., Sathyendranath, S., Seneviratne, S. I., Sörensson, A. A., Szopa, S., Takayabu, I., Tréguier, A.-M., van den Hurk, B., Vautard, R., von Schuckmann, K., Zaehle, S., Zhang, X., and Zickfeld, K.: 2021: Technical Summary, in: *Climate Change 2021: The Physical Science Basis. Contribution of Working Group I to the Sixth Assessment Report of the Intergovernmental Panel on Climate Change*, edited by: Masson-Delmotte, V., Zhai, P., Pirani, A., Connors, S. L., Péan, C., Berger, S., Caud, N., Chen, Y., Goldfarb, L., Gomis, M. I., Huang, M., Leitzell, K., Lonnoy, E., Matthews,
- 620  
625  
630



- J. B. R., Maycock, T. K., Waterfield, T., Yelekcı, O., Yu, R., and Zhou, B., Cambridge University Press, Cambridge, United Kingdom and New York, NY, USA, 33-144, 10.1017/9781009157896.002, 2021.
- Asseng, S. and van Herwaarden, A. F.: Analysis of the benefits to wheat yield from assimilates stored prior to grain filling in a range of environments, *Plant and Soil*, 256, 217-229, 10.1023/a:1026231904221, 2003.
- 635 Asseng, S., Ewert, F., Martre, P., Rotter, R. P., Lobell, D. B., Cammarano, D., Kimball, B. A., Ottman, M. J., Wall, G. W., White, J. W., Reynolds, M. P., Alderman, P. D., Prasad, P. V. V., Aggarwal, P. K., Anothai, J., Basso, B., Biernath, C., Challinor, A. J., De Sanctis, G., Doltra, J., Fereres, E., Garcia-Vile, M., Gayler, S., Hoogenboom, G., Hunt, L. A., Izaurrealde, R. C., Jabloun, M., Jones, C. D., Kersebaum, K. C., Koehler, A. K., Muller, C., Kumar, S. N., Nendel, C., O'Leary, G., Olesen, J. E., Palosuo, T., Priesack, E., Rezaei, E. E., Ruane, A. C., Semenov, M. A.,
- 640 Shcherbak, I., Stockle, C., Stratonovitch, P., Streck, T., Supit, I., Tao, F., Thorburn, P. J., Waha, K., Wang, E., Wallach, D., Wolf, I., Zhao, Z., and Zhu, Y.: Rising temperatures reduce global wheat production, *Nature Climate Change*, 5, 143-147, 10.1038/nclimate2470, 2015.
- Bassu, S., Brisson, N., Durand, J. L., Boote, K., Lizaso, J., Jones, J. W., Rosenzweig, C., Ruane, A. C., Adam, M., Baron, C., Basso, B., Biernath, C., Boogaard, H., Conijn, S., Corbeels, M., Deryng, D., De Sanctis, G., Gayler, S., Grassini, P., Hatfield, J., Hoek, S., Izaurrealde, C., Jongschaap, R., Kemanian, A. R., Kersebaum, K. C., Kim, S. H., Kumar, N. S., Makowski, D., Muller, C., Nendel, C., Priesack, E., Pravia, M. V., Sau, F., Shcherbak, I., Tao, F., Teixeira, E., Timlin, D., and Waha, K.: How do various maize crop models vary in their responses to climate change factors?, *Global Change Biology*, 20, 2301-2320, 10.1111/gcb.12520, 2014.
- 645 Betzelberger, A. M., Yendrek, C. R., Sun, J. D., Leisner, C. P., Nelson, R. L., Ort, D. R., and Ainsworth, E. A.: Ozone Exposure Response for U.S. Soybean Cultivars: Linear Reductions in Photosynthetic Potential, Biomass, and Yield, *Plant Physiology*, 160, 1827-1839, 10.1104/pp.112.205591, 2012.
- Biswas, D. K., Xu, H., Li, Y. G., Ma, B. L., and Jiang, G. M.: Modification of photosynthesis and growth responses to elevated CO<sub>2</sub> by ozone in two cultivars of winter wheat with different years of release, *Journal of Experimental Botany*, 64, 1485-1496, 10.1093/jxb/ert005, 2013.
- 650 Boote, K. J. and Pickering, N. B.: Modeling photosynthesis of row crop canopies, *Hortscience*, 29, 1423-1434, 10.21273/hortsci.29.12.1423, 1994.
- 655 Calabrese, E. J.: Hormesis: a fundamental concept in biology, *Microbial Cell*, 1, 145-149, 10.15698/mic2014.05.145, 2014.
- Choquette, N. E., Ainsworth, E. A., Bezodis, W., and Cavanagh, A. P.: Ozone tolerant maize hybrids maintain Rubisco content and activity during long-term exposure in the field, *Plant Cell and Environment*, 43, 3033-3047, 10.1111/pce.13876, 2020.
- 660 Cooper, O. R., Parrish, D. D., Ziemke, J., Balashov, N. V., Cupeiro, M., Galbally, I. E., Gilge, S., Horowitz, L., Jensen, N. R., Lamarque, J.-F., Naik, V., Oltmans, S. J., Schwab, J., Shindell, D. T., Thompson, A. M., Thouret, V., Wang, Y., and Zbinden, R. M.: Global distribution and trends of tropospheric ozone: An observation-based review, *Elementa Science of the Anthropocene*, 2, <http://doi.org/10.12952/journal.elementa.000029>, 2014.
- 665 Elliott, J., Kelly, D., Chryssanthacopoulos, J., Glotter, M., Jhunjhnuwala, K., Best, N., Wilde, M., and Foster, I.: The parallel system for integrating impact models and sectors (pSIMS), *Environmental Modelling & Software*, 62, 509-516, 10.1016/j.envsoft.2014.04.008, 2014.
- Emberson, L.: Effects of ozone on agriculture, forests and grasslands, *Philosophical Transactions of the Royal Society a-Mathematical Physical and Engineering Sciences*, 378, 27, 10.1098/rsta.2019.0327, 2020.
- 670 Emberson, L. D., Pleijel, H., Ainsworth, E. A., van den Berg, M., Ren, W., Osborne, S., Mills, G., Pandey, D., Dentener, F., Buker, P., Ewert, F., Koeble, R., and Van Dingenen, R.: Ozone effects on crops and consideration in crop models, *European Journal of Agronomy*, 100, 19-34, 10.1016/j.eja.2018.06.002, 2018.
- Feng, Z. Z. and Kobayashi, K.: Assessing the impacts of current and future concentrations of surface ozone on crop yield with meta-analysis, *Atmospheric Environment*, 43, 1510-1519, 10.1016/j.atmosenv.2008.11.033, 2009.
- 675 Feng, Z. Z., Xu, Y. S., Kobayashi, K., Dai, L. L., Zhang, T. Y., Agathokleous, E., Calatayud, V., Paoletti, E., Mukherjee, A., Agrawal, M., Park, R. J., Oak, Y. J., and Yue, X.: Ozone pollution threatens the production of major staple crops in East Asia, *Nature Food*, 3, 47-+, 10.1038/s43016-021-00422-6, 2022.
- Griffiths, P. T., Murray, L. T., Zeng, G., Shin, Y. M., Abraham, N. L., Archibald, A. T., Deushi, M., Emmons, L. K., Galbally, I. E., Hassler, B., Horowitz, L. W., Keeble, J., Liu, J., Moeini, O., Naik, V., O'Connor, F. M., Oshima, N., Tarasick, D., Tilmes, S., Turnock, S. T., Wild, O., Young, P. J., and Zanis, P.: Tropospheric ozone in CMIP6 simulations, *Atmospheric Chemistry and Physics*, 21, 4187-4218, 10.5194/acp-21-4187-2021, 2021.
- 680 Guarin, J. R., Kassie, B., Mashaheet, A. M., Burkey, K., and Asseng, S.: Modeling the effects of tropospheric ozone on wheat growth and yield, *European Journal of Agronomy*, 105, 13-23, 10.1016/j.eja.2019.02.004, 2019.
- 685 Heck, W. W., Cure, W. W., Rawlings, J. O., Zaragoza, L. J., Heagle, A. S., Heggstad, H. E., Kohut, R. J., Kress, L. W., and Temple, P. J.: Assessing impacts of ozone on agricultural crops: 2. Crop yield functions and alternative



- exposure statistics, *Journal of the Air Pollution Control Association*, 34, 810-817, 10.1080/00022470.1984.10465815, 1984.
- 690 Hoogenboom, G., Porter, C. H., Boote, K. J., Shelia, V., Wilkens, P. W., Singh, U., White, J. W., Asseng, S., Lizaso, J. I., Moreno, L. P., Pavan, W., Ogoshi, R., Hunt, L. A., Tsuji, G. Y., and Jones, J. W.: The DSSAT crop modeling ecosystem, in: *Advances in Crop Modeling for a Sustainable Agriculture*, edited by: Boote, K. J., Burleigh Dodds Science Publishing, Cambridge, United Kingdom, 173-216, 10.19103/AS.2019.0061.10, 2019.
- Hou, P. and Wu, S. L.: Long-term Changes in Extreme Air Pollution Meteorology and the Implications for Air Quality, *Scientific Reports*, 6, 9, 10.1038/srep23792, 2016.
- 695 Hunsaker, D. J., Kimball, B. A., Pinter, P. J., LaMorte, R. L., and Wall, G. W.: Carbon dioxide enrichment and irrigation effects on wheat evapotranspiration and water use efficiency, *Transactions of the Asae*, 39, 1345-1355, 1996.
- IPCC: *Climate Change 2021: The Physical Science Basis. Contribution of Working Group I to the Sixth Assessment Report of the Intergovernmental Panel on Climate Change*, 2021.
- 700 Jagermeyr, J., Muller, C., Ruane, A. C., Elliott, J., Balkovic, J., Castillo, O., Faye, B., Foster, I., Folberth, C., Franke, J. A., Fuchs, K., Guarin, J. R., Heinke, J., Hoogenboom, G., Iizumi, T., Jain, A. K., Kelly, D., Khabarov, N., Lange, S., Lin, T. S., Liu, W. F., Mialyk, O., Minoli, S., Moyer, E. J., Okada, M., Phillips, M., Porter, C., Rabin, S. S., Scheer, C., Schneider, J. M., Schyns, J. F., Skalsky, R., Smerald, A., Stella, T., Stephens, H., Webber, H., Zabel, F., and Rosenzweig, C.: Climate impacts on global agriculture emerge earlier in new generation of climate and crop models, *Nature Food*, 2, 875+, 10.1038/s43016-021-00400-y, 2021.
- 705 Jones, C. A. and Kiniry, J. R.: *CERES-Maize: A simulation model of maize growth and development*, Texas A&M University Press, College Station, TX1986.
- Jones, J. W., Hoogenboom, G., Porter, C. H., Boote, K. J., Batchelor, W. D., Hunt, L. A., Wilkens, P. W., Singh, U., Gijssman, A. J., and Ritchie, J. T.: The DSSAT cropping system model, *European Journal of Agronomy*, 18, 235-265, 10.1016/s1161-0301(02)00107-7, 2003.
- 710 Khan, S. and Soja, G.: Yield responses of wheat to ozone exposure as modified by drought-induced differences in ozone uptake, *Water Air and Soil Pollution*, 147, 299-315, 10.1023/a:1024577429129, 2003.
- Kimball, B. A., LaMorte, R. L., Pinter, P. J., Wall, G. W., Hunsaker, D. J., Adamsen, F. J., Leavitt, S. W., Thompson, T. L., Matthias, A. D., and Brooks, T. J.: Free-air CO<sub>2</sub> enrichment and soil nitrogen effects on energy balance and evapotranspiration of wheat, *Water Resources Research*, 35, 1179-1190, 10.1029/1998wr900115, 1999.
- 715 Kimball, B. A., Pinter Jr., P. J., LaMorte, R. L., Leavitt, S. W., Hunsaker, D. J., Wall, G. W., Wechsung, F., Wechsung, G., Bloom, A. J., and White, J. W.: Data from the Arizona FACE (free-air CO<sub>2</sub> enrichment) experiments on wheat at ample and limiting levels of water and nitrogen, *Open Data Journal for Agricultural Research*, 3, 29-38, <https://doi.org/10.18174/odjar.v3i1.15826>, 2017.
- 720 Kothari, K., Battisti, R., Boote, K. J., Archontoulis, S. V., Confalone, A., Constantin, J., Cuadra, S. V., Debaeke, P., Faye, B., Grant, B., Hoogenboom, G., Jing, Q., van der Laan, M., da Silva, F. A. M., Marin, F. R., Nehbandani, A., Nendel, C., Purcell, L. C., Qian, B. D., Ruane, A. C., Schoving, C., Silva, E., Smith, W., Soltani, A., Srivastava, A., Vieira, N. A., Slone, S., and Salmeron, M.: Are soybean models ready for climate change food impact assessments?, *European Journal of Agronomy*, 135, 15, 10.1016/j.eja.2022.126482, 2022.
- 725 Lesser, V. M., Rawlings, J. O., Spruill, S. E., and Somerville, M. C.: Ozone effects on agricultural crops: Statistical methodologies and estimated dose-response relationships, *Crop Science*, 30, 148-155, 10.2135/cropsci1990.0011183X003000010033x, 1990.
- Leung, F., Williams, K., Sitch, S., Tai, A. P. K., Wiltshire, A., Gornall, J., Ainsworth, E. A., Arkebauer, T., and Scoby, D.: Calibrating soybean parameters in JULES 5.0 from the US-Ne2/3 FLUXNET sites and the SoyFACE-O-3 experiment, *Geoscientific Model Development*, 13, 6201-6213, 10.5194/gmd-13-6201-2020, 2020.
- 730 Li, T., Hasegawa, T., Yin, X. Y., Zhu, Y., Boote, K., Adam, M., Bregaglio, S., Buis, S., Confalonieri, R., Fumoto, T., Gaydon, D., Marcaida, M., Nakagawa, H., Oriol, P., Ruane, A. C., Ruget, F., Singh, B., Singh, U., Tang, L., Tao, F. L., Wilkens, P., Yoshida, H., Zhang, Z., and Bouman, B.: Uncertainties in predicting rice yield by current crop models under a wide range of climatic conditions, *Global Change Biology*, 21, 1328-1341, 10.1111/gcb.12758, 2015.
- 735 Mills, G., Sharps, K., Simpson, D., Pleijel, H., Frei, M., Burkey, K., Emberson, L., Uddling, J., Broberg, M., Feng, Z. Z., Kobayashi, K., and Agrawal, M.: Closing the global ozone yield gap: Quantification and cobenefits for multistress tolerance, *Global Change Biology*, 24, 4869-4893, 10.1111/gcb.14381, 2018a.
- Mills, G., Sharps, K., Simpson, D., Pleijel, H., Broberg, M., Uddling, J., Jaramillo, F., Davies, W. J., Dentener, F., Van den Berg, M., Agrawal, M., Agrawal, S. B., Ainsworth, E. A., Buker, P., Emberson, L., Feng, Z. Z., Harmens, H., Hayes, F., Kobayashi, K., Paoletti, E., and Van Dingenen, R.: Ozone pollution will compromise efforts to increase global wheat production, *Global Change Biology*, 24, 3560-3574, 10.1111/gcb.14157, 2018b.
- 740





- Morris, M. D.: Factorial sampling plans for preliminary computational experiments, *Technometrics*, 33, 161-174, 10.2307/1269043, 1991.
- 745 NRCS, S. S. S.: Natural Resources Conservation Service, United States Department of Agriculture. Web Soil Survey, 2023.
- Osborne, S. A., Mills, G., Hayes, F., Ainsworth, E. A., Buker, P., and Emberson, L.: Has the sensitivity of soybean cultivars to ozone pollution increased with time? An analysis of published dose-response data, *Global Change Biology*, 22, 3097-3111, 10.1111/gcb.13318, 2016.
- 750 R Core Team: R: a language and environment for statistical computing, 2023.
- Ritchie, J. T., Alocilja, E. C., Singh, U., and Uehara, G.: IBSNAT and the CERES-RICE model, in: *Weather and Rice, Proceedings of the International Workshop on The Impact of Weather Parameters on Growth and Yield of Rice*, IRRI, Philippines, 271-283, 1987.
- 755 Rosenzweig, C., Jones, J. W., Hatfield, J. L., Ruane, A. C., Boote, K. J., Thorburne, P., Antle, J. M., Nelson, G. C., Porter, C., Janssen, S., Asseng, S., Basso, B., Ewert, F., Wallach, D., Baigorria, G., and Winter, J. M.: The Agricultural Model Intercomparison and Improvement Project (AgMIP): Protocols and pilot studies, *Agricultural and Forest Meteorology*, 170, 166-182, 10.1016/j.agrformet.2012.09.011, 2013.
- Sampedro, J., Waldhoff, S. T., Van de Ven, D. J., Pardo, G., Van Dingenen, R., Arto, I., del Prado, A., and Sanz, M. J.: Future impacts of ozone driven damages on agricultural systems, *Atmospheric Environment*, 231, 11, 10.1016/j.atmosenv.2020.117538, 2020.
- 760 Schauburger, B., Rolinski, S., Schaphoff, S., and Muller, C.: Global historical soybean and wheat yield loss estimates from ozone pollution considering water and temperature as modifying effects, *Agricultural and Forest Meteorology*, 265, 1-15, 10.1016/j.agrformet.2018.11.004, 2019.
- 765 Schiferl, L. D. and Heald, C. L.: Particulate matter air pollution may offset ozone damage to global crop production, *Atmospheric Chemistry and Physics*, 18, 5953-5966, 10.5194/acp-18-5953-2018, 2018.
- Simpson, D., Arneth, A., Mills, G., Solberg, S., and Uddling, J.: Ozone - the persistent menace: interactions with the N cycle and climate change, *Current Opinion in Environmental Sustainability*, 9-10, 9-19, 10.1016/j.cosust.2014.07.008, 2014.
- 770 Szopa, S., Naik, V., Adhikary, B., Artaxo, P., Bernsten, T., Collins, W. D., Fuzzi, S., Gallardo, L., Kiendler-Scharr, A., Klimont, Z., Liao, H., Unger, N., and Zanis, P.: 2021: Short-Lived Climate Forcers, in: *Climate Change 2021: The Physical Science Basis. Contribution of Working Group I to the Sixth Assessment Report of the Intergovernmental Panel on Climate Change*, edited by: Masson-Delmotte, V., Zhai, P., Pirani, A., Connors, S. L., Péan, C., Berger, S., Caud, N., Chen, Y., Goldfarb, L., Gomis, M. I., Huang, M., Leitzell, K., Lonnoy, E., Matthews, J. B. R., Maycock, T. K., Waterfield, T., Yelekçi, O., Yu, R., and Zhou, B., Cambridge University Press, Cambridge, United Kingdom and New York, NY, USA, 817-922, 10.1017/9781009157896.008, 2021.
- 775 Tai, A. P. K., Sadiq, M., Pang, J. Y. S., Yung, D. H. Y., and Feng, Z. Z.: Impacts of Surface Ozone Pollution on Global Crop Yields: Comparing Different Ozone Exposure Metrics and Incorporating Co-effects of CO<sub>2</sub>, *Frontiers in Sustainable Food Systems*, 5, 18, 10.3389/fsufs.2021.534616, 2021.
- 780 Toreti, A., Deryng, D., Tubiello, F. N., Muller, C., Kimball, B. A., Moser, G., Boote, K., Asseng, S., Pugh, T. A. M., Vanuytrecht, E., Pleijel, H., Webber, H., Durand, J. L., Dentener, F., Ceglar, A., Wang, X. H., Badeck, F., Lecerf, R., Wall, G. W., van den Berg, M., Hoegy, P., Lopez-Lozano, R., Zampieri, M., Galmarini, S., O'Leary, G. J., Manderscheid, R., Contreras, E. M., and Rosenzweig, C.: Narrowing uncertainties in the effects of elevated CO<sub>2</sub> on crops, *Nature Food*, 1, 775-782, 10.1038/s43016-020-00195-4, 2020.
- 785 USDA NASS: Field crops usual planting and harvest dates (October 2010), 2010.
- Wang, X. P. and Mauzerall, D. L.: Characterizing distributions of surface ozone and its impact on grain production in China, Japan and South Korea: 1990 and 2020, *Atmospheric Environment*, 38, 4383-4402, 10.1016/j.atmosenv.2004.03.0367, 2004.
- Wickham, H.: *ggplot2: elegant graphics for data analysis*, 2016.
- 790 Wickham, H., François, R., Henry, L., Müller, K., and Vaughan, D.: *dplyr: a grammar of data manipulation. R package version 1.1.2*, 2023.
- Wilkerson, G. G., Jones, J. W., Boote, K. J., Ingram, K. T., and Mishoe, J. W.: Modeling soybean growth for crop management, *Transactions of the Asae*, 26, 63-73, 1983.
- Xia, L. L., Lam, S. K., Kiese, R., Chen, D. L., Luo, Y. Q., van Groenigen, K. J., Ainsworth, E. A., Chen, J., Liu, S. W., Ma, L., Zhu, Y. H., and Butterbach-Bahl, K.: Elevated CO<sub>2</sub> negates O<sub>3</sub> impacts on terrestrial carbon and nitrogen cycles, *One Earth*, 4, 1752-1763, 10.1016/j.oneear.2021.11.009, 2021.
- 795 Zhang, Y. Z. and Wang, Y. H.: Climate-driven ground-level ozone extreme in the fall over the Southeast United States, *Proceedings of the National Academy of Sciences of the United States of America*, 113, 10025-10030, 10.1073/pnas.1602563113, 2016.